United States
Department of
Agriculture

Forest Service

Forest
Products
Laboratory

Research
Paper
FPL–RP–554

Strength and Stiffness of Reinforced Yellow-Poplar Glued-Laminated Beams

Roland Hernandez
Julio F. Davalos
Somnath S. Sonti
Youngchan Kim
Russell C. Moody

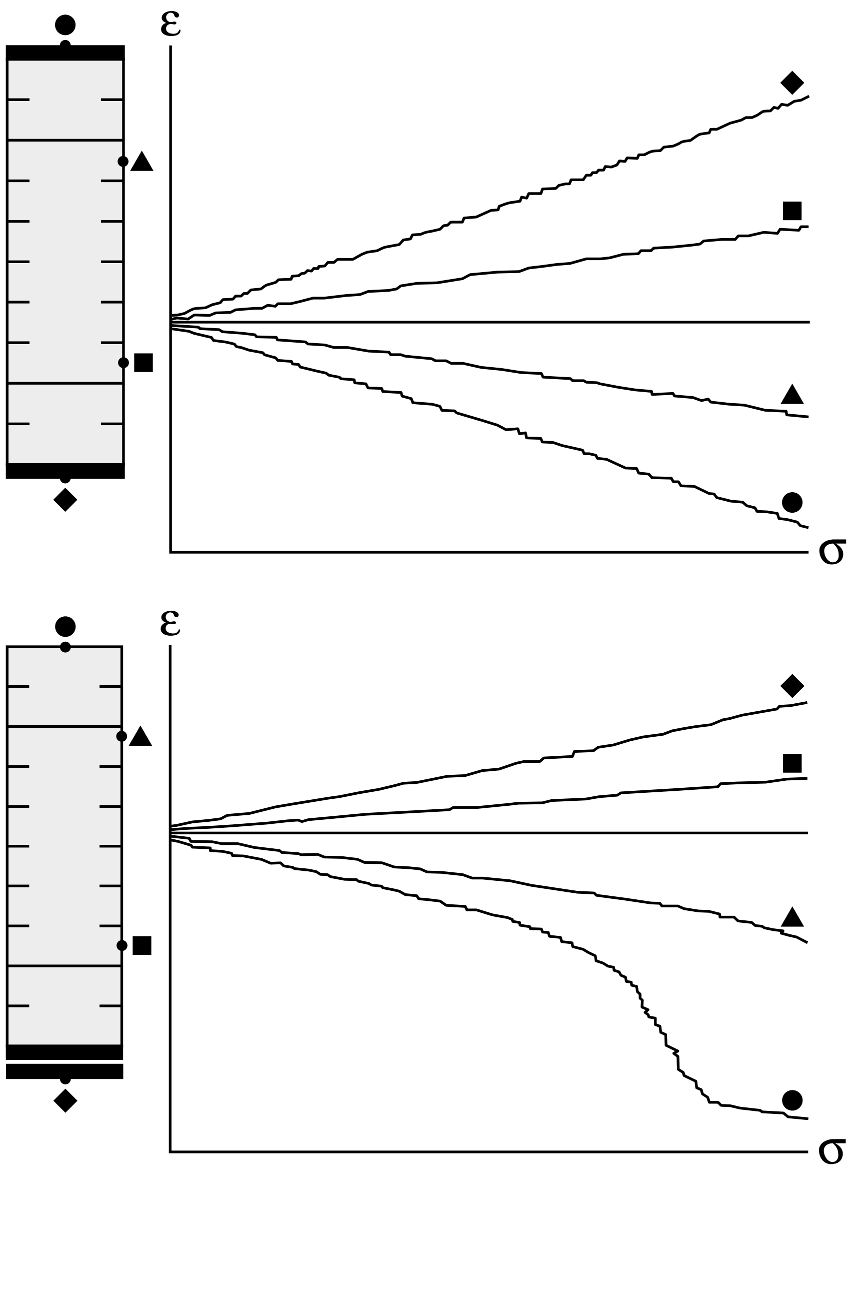

Abstract

In bridge applications, it is often necessary to minimize the depth of the bridge structure to provide for the required hydraulic opening or reduce the volume of approach fill. For bridges that utilize structural glued-laminated (glulam) timber beams as stringers, reinforcement using thin strips of pultruded E-glass-fiber-reinforced plastic (GFRP) composites may permit reduced depth, because the reinforcement has the potential to increase stiffness and strength. This study is part of an overall effort aimed at evaluating the potential for commercial production of glulam-GFRP beams in current wood-laminating plants and a wood adhesive compatible with existing equipment. Twelve Yellow-Poplar glulam GFRP beams were commercially manufactured, and their performance was evaluated. The GFRP panels were bonded to the wood with a resorcinol formaldehyde adhesive to provide the reinforcement. The simplicity of the process used to manufacture the test beams indicates that the commercial production of glulam-GFRP beams is feasible. Increases of 18 percent in stiffness and 26 percent in strength were achieved by adding 3 percent of GFRP by volume. The bending strength values of the beams predicted by the ASTM D3737 procedure correlate well with the experimental values. However, the observed delamination of the reinforcement indicates that improved bonding strength of wood–GFRP interfaces is needed. Results of this study will be useful to manufacturers interested in improving the performance of glulam timber beams.

Keywords: Glulam, fiber-reinforced plastic, Yellow-Poplar, composites

July 1997

Hernandez, Roland; Davalos, Julio F.; Sonti, Somnath S.; Kim, Youngchan; Moody, Russell C. 1997. Strength and stiffness of reinforced Yellow-Poplar glued-laminated beams. Res. Pap. FPL–RP–554. Madison, WI: U.S. Department of Agriculture, Forest Service, Forest Products Laboratory. 28 p.

A limited number of free copies of this publication are available to the public from the Forest Products Laboratory, One Gifford Pinchot Drive, Madison, WI 53705–2398. Laboratory publications are sent to more than 1,000 libraries in the United States and elsewhere.

The Forest Products Laboratory is maintained in cooperation with the University of Wisconsin.

Acknowledgments

We thank Creative Pultrusions, Inc., for providing the fiber-reinforced plastic laminates, Indspec Chemical Corporation for providing the adhesives, and Unit Structures for manufacturing the glued-laminated beams.

Contents

Page

Strength and Stiffness of Reinforced Yellow-Poplar Glued-Laminated Beams

Roland Hernandez, Research General Engineer
Forest Products Laboratory, Madison, Wisconsin

Julio F. Davalos, Associate Professor
Somnath S. Sonti, Research Engineer
Youngchan Kim, Graduate Research Assistant
Department of Civil and Environmental Engineering
West Virginia University, Morgantown, West Virginia

Russell C. Moody, Supervisory Research General Engineer
Forest Products Laboratory, Madison, Wisconsin

Introduction

The abundance and underutilization of Yellow-Poplar lumber in the regions of Virginia and West Virginia provide a potential resource for a variety of structural applications. Long-span, glued-laminated (glulam) beams are currently needed for timber bridges in these regions. Although structural glulam timbers are produced primarily from Southern Pine and Douglas Fir lumber, Moody and others (1993) recently showed that Yellow-Poplar beams can be manufactured with comparable engineering properties to those of softwoods. As a result, standards for Yellow-Poplar glulam timber beam combinations with stiffness and strength properties comparable to softwoods are being incorporated by the American Institute of Timber Construction (AITC) into the hardwood glulam standard (AITC 1996). For some bridge applications, it is important to minimize the depth of the superstructure to provide for the needed hydraulic opening or minimize the volume of fill in the approaches. By reinforcing glulam timber with a material that has a high level of stiffness and strength, the required depth of the bridge stringers can be reduced and an increase in bending stiffness and strength can be achieved.

Background

Previous researchers have studied the feasibility of reinforcing glulam beams with metals and fiber-reinforced plastics. Spaun (1981) presented reviews of previous work on the reinforcement of wood with other materials. Metal reinforcements included aluminum and steel; various adhesive systems and mechanical fasteners were used to attach the metal reinforcements. Mark (1961) used a formaldehyde adhesive to bond aluminum strips, coated with casein-latex primer, to wood cores. Failure of the beams occurred mainly by separation and buckling of the aluminum facings. Similarly, Peterson (1965) reinforced wood beams with pretensioned steel strips. Lantos (1970) used round steel bars to reinforce wood beams. Curtis (1972) used steel-plate reinforcement that extended through the entire depth of wood beams, a method called the flitch plate beam design, and obtained a 12- to 31-percent increase in stiffness but no increase in strength. Krueger and Sandberg (1974) reported on ultimate strength design of Southern Pine reinforced on the tension side with a bronze-coated woven steel wire, which was bonded with epoxy. The beams exhibited compression failures.

Fibrous composite reinforcements were also used by several researchers. Theakston (1965) used resin-preimpregnated fiberglass reinforcements bonded with epoxy. The beams showed a 39-percent increase in bending strength. Spaun (1981) selected E-glass fiber rovings for reinforcement because of its low cost and phenol-resorcinol adhesive for all gluelines. He observed significant increases in tensile strength in proportion to the fiber-volume fraction of the E-glass reinforcement. Tingley (1994) described a method of reinforcing glulam timber using aramid fiber and glass-reinforced laminates. Plevris and Triantofillou (1992) studied the response of wood beams reinforced with thin layers of carbon-fiber-reinforced plastic composites. Triantofillou and Deskovic (1992) used prestressed carbon-fiber-reinforced plastic sheets as external reinforcements of wood beams. More recently, Leichti and others (1993) reported on the future installation of aramid fiber reinforced glulam members for a pedestrian bridge in Oregon.

The initial efforts of using hand lay-up, resin-impregnated fibers cured on top of the wood laminate indicated that the procedure was suitable for large-scale production of reinforced wood beams. Thus, current research on wood reinforcement has focused on the use of fiber-reinforced strips bonded to wood laminates (Western Wood Structures 1994). Additional information is needed to develop specifications and design values for fiber-reinforced plastic glulam timber.

Objective And Scope

The overall objective of this study was to evaluate the performance of Yellow-Poplar glulam beams reinforced with E-glass-fiber-reinforced plastic/vinylester (GFRP) composite sheets. Specific objectives were to (1) demonstrate a fabrication process for glulam-GFRP composite beams that can be implemented in current glulam plants without significant changes to existing processing operations, (2) demonstrate the significant increases that can be achieved in stiffness and strength of glulam beams reinforced with a small percentage of GFRP, and (3) determine if the existing ASTM standard for glulam timber can be adapted to predict the linear and failure response of glulam-GFRP beams.

Twelve Yellow-Poplar glulam beams of approximately 4 in. by 13 in. by 20 ft were fabricated and reinforced with GFRP at a glulam plant. (See Table 1 for metric conversion factors.) For half the beams, two layers of GFRP were bonded to the bottom (tensile) surface of the glulam beams. For the other half, one layer was bonded to both the top and bottom surfaces of the beams. The GFRP-to-wood interface was bonded with a modified resorcinol formaldehyde wood adhesive, which was compatible with existing manufacturing processes and previously shown to provide acceptable bonding characteristics (Munipalle 1992). The GFRP-to-GFRP interface was bonded with an epoxy-based adhesive.

The study presented here focuses on using a low-cost and mass-produced reinforcement with a high level of stiffness and strength to manufacture glulam-FRP beams in commercial plants.

Research Methodology

The procedures used in conducting this study were organized in four parts: (1) beam design, (2) material selection and characterization, (3) finger joint and beam manufacture, and (4) evaluation procedures.

Table 1—SI conversion factors

English unit	Conversion factor	SI unit
inch (in.)	25.4	millimeter (mm)
in/in·lb	2.22046	m/m•kg
Fahrenheit (°F)	(°F − 32)/1.8	Celsius (°C)
foot (ft)	0.3048	meter (m)
lb/in^2 (stress)	6,894	pascal (Pa)
lb/ft^2	4.88	kilogram/meter^2 (kg/m^2)

Beam Design

The design of the beams was based on information obtained from a previous study on the use of E-rated Yellow-Poplar lumber for glulam timber (Moody and others 1993). The approach was to manufacture glulam beams similar to those previously evaluated and add the GFRP to the outside of these beams. The intended thickness of the GFRP panels produced beams with approximately 2.8-percent GFRP by volume. Properties of the beams without the GFRP were predicted using ASTM D3737 procedures. These procedures were modified to predict the strength and stiffness properties of the reinforced beams. Input parameters for the D3737 analysis are given in Table 2.

Conventional Beam

The beam layup shown in Figure 1, which is similar to that previously evaluated by Moody and others (1993), was selected. E-rated lumber having an average modulus of elasticity (MOE) of 2.0×10^6 lb/in^2 was used for the top and bottom 20 percent of the beam cross section. Visual criteria applied to the E-rated lumber included an allowable maximum edge-knot (EK) of 1/6 the width of the lumber for the laminations on the tension side of the beams and a 1/3 EK restriction for the laminations on the compression side of the beams. The remaining 60 percent of the core laminations was made with No. 2 visual grade Yellow-Poplar lumber. Analyses using ASTM D3737 indicated that a 10-lamination beam would have an MOE of 1.80×10^6 lb/in^2 and design stress in bending of 2,500 lb/in^2 if a special tension lamination was used and a design stress in bending of 2,200 lb/in^2 without the special tension lamination. Yellow-Poplar beams of Moody and others (1993) had a design stress of 2,650 lb/in^2.

Reinforced Beam

The transformed section analysis portion of the D3737 procedure was modified to determine the effect of adding either (a) two 3/16-in. pieces of GFRP (2.8 percent) to the bottom

Table 2—Assumed properties of Yellow-Poplar lumber and GFRP for analysis using ASTM D3737

Lumber grade	MOE ($\times 10^6$ lb/in^2)	$\bar{x}$[a] (%)	$\bar{x}$ + h[b] (%)	Bending stress index (lb/in^2)
2.0E–1/6	2.0	3.0	27	3,250
2.0E–1/3	2.0	5.0	30	3,250
No. 2	1.5	8.0	42	1,910
GFRP	0.0	0.0	0.0	35,000

[a] $\bar{x}$ is the average of the sum of all knot sizes, within each 1-ft length, taken at 0.2-ft intervals and expressed as a percentage of the lumber cross section.
[b] $\bar{x}$ + h is equal to the 99.5 percentile knot size (ASTM 1992a).

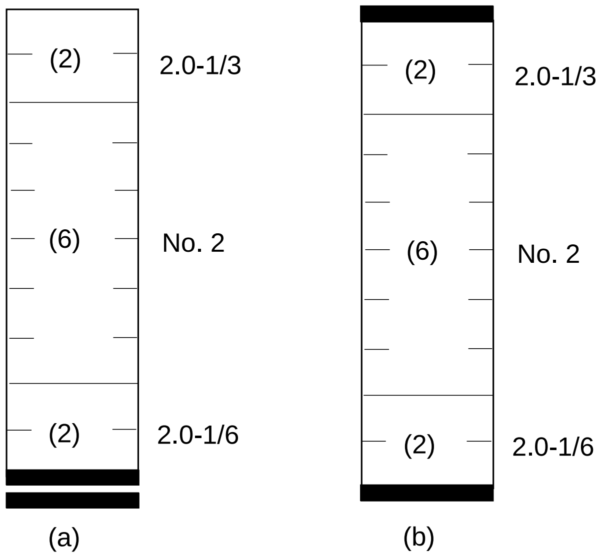

Figure 1—Illustration of Yellow-Poplar glulam beams with GFRP laminations: (a) two pieces of GFRP used as bottom tension plies and (b) single piece of GFRP used as outer tension and compression ply.

of the beam or (b) one 3/16-in. piece to the top and bottom of the beams (1.4 percent on both the top and bottom).

Based on tests, an MOE of 6.0×10^6 lb/in^2 was used for the GFRP. Lamination thickness was 1.3 in. for the wood, so each piece of GFRP was analyzed with a thickness of 0.144 laminations for the D3737 analysis. The effect of the GFRP layers on the glulam beam stiffness was easily calculated using this procedure. However, the effect on design stress required assumptions. These were that the strength of the GFRP was not critical and the design bending stress in the lumber would control the design bending stress for the glulam-GFRP beam. Thus, a bending stress index of about 10 times that of the 2.0E lumber was assigned to the GFRP.

Results of the analysis are given in Table 3, with the predicted increases in both strength and stiffness by using either two 3/16-in. layers of the GFRP on the bottom or one on both the top and bottom. In all analyses, the controlling design bending stress for the beams was the lowest of those calculated in the following four locations: outer tension zone (wood), outer compression zone (wood), No. 2 lumber on the tension side of the beam, or No. 2 lumber on the compression side of the beam. For the combination with reinforcement on top and bottom, the analyses indicated that the controlling location was nearly balanced between either the 2.0–1/6 lumber on the tension side or the No. 2 lumber in the third lamination from the tension side. For the combination with reinforcement on the bottom only, the analysis indicated that a close balance between the design bending stress was calculated for all four locations (all within less than 5 percent). Thus, some compression failures would be predicted based on ASTM D3737 procedures. Special tension laminations were not used, because the GFRP fulfilled the strength requirements specified by ASTM D3737.

Table 3—Predicted properties of the glulam beams, both unreinforced and reinforced with GFRP

Identification	Predicted MOE	Ratio to unreinforced	Predicted design stress	Ratio to unreinforced
Unreinforced	1.80	1.00	2,500	1.00
Bottom only	2.09	1.16	3,400	1.36
Top and bottom	2.12	1.18	3,000	1.20

For the combination with reinforcement on the bottom only, the neutral axis was predicted to shift slightly toward the tension side so that it was located at 46.9 percent of the depth from the tension side, rather than at 50 percent (mid-depth) for the balanced beams.

Material Selection and Characterization

This section describes the characteristics of the material (GFRP, lumber, and adhesive) used in this study and the methods used to evaluate material properties.

Material Selection

Pultruded GFRP was selected for the reinforcement of the glulam beams. The GFRP composite used in this study consisted of E-glass rovings embedded in a Vinylester matrix. The E-glass rovings provide the longitudinal strength for the product, and the resin binds the fibers together to provide shear strength, corrosion resistance, and other properties. E-glass was selected because of its cost competitiveness and mass production capabilities. The GFRP laminates used in this study consisted of 4-in. by 0.1875-in. by 20-ft plates with a fiber-volume fraction of 60 percent. The rovings were 100 percent aligned parallel to the beam span.

Yellow-Poplar lumber was custom sawn from logs grown in West Virginia and surfaced on the two faces. Lumber thickness was nominal 2 in.; actual widths varied from 4.5 to 7.0 in. Approximately 12,000 lineal ft of lumber was visually graded into either Select Structural (SS) or No. 2, using nationally recognized grading rules (NELMA 1991). The lumber was then kiln dried to an equilibrium moisture content of 12 percent and transported to the laminating plant.

The E-rated lumber grades targeted in Table 2 were required to meet both the MOE criteria in AITC 117–Manufacturing (AITC 1993) and the specified EK criteria. To meet these requirements, the SS and No. 2 grade lumber were first divided into one of three visual categories: (1) pieces having an EK occupying up to 1/6 of the lumber width, (2) pieces having an EK between 1/6 and 1/3 the lumber width, and (3) all remaining pieces that exceeded the 1/3 EK criteria, which would be designated as No. 2 grade material. Edge-knot grading was based on the actual width of the lumber. Because of the varying lumber widths, the final EK sizes of the finished beams were difficult to estimate.

We planned to measure MOE using commercially available equipment based on transverse-vibration nondestructive techniques (Ross and others 1991). Long-span static bending deflection readings would then be taken at random throughout the testing to verify transverse vibration determinations of MOE. A typical target sample size for this calibration group of lumber was approximately 50 specimens, and past research has shown that a coefficient of determination (r^2) of greater than 0.9 should be expected between results of the two types of tests. Because the lumber was only surfaced on the faces, the lumber width sometimes varied from end-to-end by as much as 1.5 in. For this reason, transverse vibration methods were not always possible, because these measurements are based on the assumption of uniform width, thickness, and density along the length of the member. To ensure accurate determination of lumber MOE, all lumber designated for the two E-rated grades listed in Table 2 was tested using a static deflection method. Dynamic MOE was determined for a representative group of the No. 2 grade lumber. Static deflection tests were randomly conducted for this smaller group of No. 2 grade lumber to verify proper calibration of the transverse vibration equipment.

When the 1/6 EK, 1/3 EK, and No. 2 grade lumber were visually sorted and tested for MOE, the 1/6 and 1/3 EK groups were manually sorted to obtain the target average MOE values listed in Table 2. No sorting based on MOE was conducted with the No. 2 grade lumber. The sorting scheme used to achieve the target MOE distributions is given in Table 4.

The adhesive for bonding the GFRP to the wood was a two-component resorcinol-formaldehyde resin that had cured at room temperature. The two parts of the adhesive were resorcinol-formaldehyde polymer, which is a liquid resin, and paraformaldehyde, which is a powdered hardener. The two parts were mixed in the ratio of 5 parts resin to 1 part hardener (by weight). The adhesive met the requirements of ANSI/AITC A190.1 (ANSI 1992). It has also been shown that this adhesive can provide an adequate bond between Yellow-Poplar and GFRP (Gardner and others 1994, Barbero and others 1994).

Table 4—Target MOE values and sorting scheme

Lamination grade	Sorting and grading criteria
2.0–1/6	Average MOE of 2.0 to 2.1 $\times$ 10^6 lb/in^2 No MOE less than 1.60 $\times$ 10^6 lb/in^2 5th percentile at 1.67 $\times$ 10^6 lb/in^2 No MOE greater than 2.4 $\times$ 10^6 lb/in^2 Maximum EK size of 1/6 the lumber width
2.0–1/3	MOE restrictions same as for 2.0E–1/6 grade Maximum EK size of 1/3 the lumber width

Epoxy was used for bonding GFRP to GFRP. This epoxy is widely used for bonding fiberglass panels to a variety of substrates. As recommended by the manufacturer, the two components of the epoxy were mixed in equal ratios by volume.

Material Characterization

Small GFRP samples were tested to obtain longitudinal tensile stiffness and strength, Poisson's ratio, and shear stiffness and strength. Lumber samples were evaluated to determine bending stiffness, and knot sizes were measured to determine their distribution for each grade.

For the GFRP material, the longitudinal tensile MOE and tensile strength were determined by testing 10 specimens (0.75 by 0.1875 by 8 in.) that were cut from the strips used for the glulam reinforcement. To avoid damage of the coupons at the grips, aluminum tabs (4 by 0.75 in.) were bonded at the ends of the specimens with epoxy adhesive. A three-element strain gage rosette was bonded to each specimen, and the longitudinal, transverse, and 45° direction strains were recorded. The specimens were tested at a 0.2-in/min loading rate. A linear regression of the load–strain data was used to obtain the longitudinal tensile MOE and Poisson’s ratio. The ultimate tensile strength was computed from the load at failure and the cross-sectional area of each specimen measured before the tests. The in-plane shear modulus and the shear strength were obtained from torsion tests of 1.25- by 0.1875- by 17-in. specimens.

The MOE properties for each lumber grade were gathered during the initial grade sorting at the laminating plant. The characterization of MOE properties for later analyses would be based on the lumber that was actually used in the glulam beams, which would be determined by mapping the lumber identification numbers as they appeared in the beams. To predict beam bending strength using ASTM D3737 procedures, knot sizes were measured for each grade of lumber (after visual and mechanical sorting). The occurrence of knots was mapped on prepared data sheets, following guidelines provided by AITC. The gathered knot information was then analyzed using procedures specified in ASTM D3737, which are based on work by Freas and Selbo (1954). Knots were measured on all 2.0E–1/6 laminations and on randomly selected samples of each the 2.0E–1/3 and No. 2 lumber grades.

Finger Joint and Beam Manufacture

When all the wood lamination grades were visually and mechanically sorted, a small sample of end joints was manufactured at the laminating plant from the sorted 2.0E–1/6 grade lumber. These end joints were manufactured 1 day prior to the manufacture of the test beams, as part of the daily quality control (QC) procedures conducted at the laminating plant. Daily QC testing of end joints intended for glulam beam manufacture is normally conducted on tension lamination-quality end joints. However, the GFRP layers in the glulam configurations targeted in this study were used as replacements for the special tension laminations; therefore, QC tests were conducted on the 2.0E–1/6 grade of end joints. For manufacture, production line speeds of 49 ft/min were used, which is typical during glulam manufacture at this laminating facility. A total of 11 end-joint specimens were manufactured and finished to a dimension of 5 in. wide by 1.375 in. thick: 10 were intended for tension tests and 1 for the glue-bond delamination test.

For glulam beam manufacture, twelve 10-lamination beams were fabricated. Reinforcement was then applied to the beams to produce two different combinations: six beams with two GFRP layers in the tension zone and six beams with one GFRP layer in each of the tension and compression zones (Fig. 1). Lumber pieces were end jointed using a melamine adhesive and cured in a radiofrequency tunnel. The end-jointed lumber was then cut into 21-ft-long laminations and stacked by grade according to the beam layup. Location of each piece of lumber in the laminated beam was recorded on beam maps.

The laminations were then processed through the final stage of the manufacturing operation. This involved planing the laminations to a final thickness of 1.3 in., spreading the adhesive on the face of the laminations, assembling the beams, and applying the required clamping pressure during curing. Following removal from the forms, the beams were planed to final dimensions of 4 in. wide, which was the largest width obtainable because of the wide variation in the lumber. The 13-in.-deep beams were cut to 20-ft lengths and visually inspected to verify conformance to ANSI/AITC A190.1 (ANSI 1992), such as proper finger-joint spacing and adequate glue bonds.

During manufacture of the glulam beams, additional laminations were produced to obtain samples of finger-jointed lumber for subsequent laboratory testing. To distinguish from the previous "QC" finger-joint specimens, these specimens will be referred to as the "test" specimens. These test specimens were manufactured during the same production run as the glulam beams. Thirty specimens from the 2.0E–1/6 grade and another 30 from the No. 2 grade were targeted for manufacture. The test specimens were approximately 8 ft long, with the finger joint within 1 ft of midlength. Each test specimen was planed to a thickness of about 1.3 in. and edged to a width of 4 in.

After manufacture and prior to testing, the test group of 2.0–1/6 end joints was re-graded to determine if some of the specimens would meet the criteria to qualify as special tension laminations. This information could be used to compare with tension lamination-quality Yellow-Poplar finger joints from past research. The tension lamination criteria for these joints included a 40-percent limitation on EK plus grain deviation on the lumber width and a center knot plus grain deviation limitation of 45 percent of the lumber width. Also, the longitudinal grain of the lumber could not exceed a 1-in-14 slope. These criteria for the 2.0–1/6 grade would allow the glulam beam configuration from Figure 1 to meet a design bending strength of approximately 2,320 lb/in^2, without the use of the GFRP.

The GFRP surfaces were sanded, then cleaned with ethanol. The top or bottom surface of the beams were also sanded before bonding. The two-part resorcinol formaldehyde adhesive was mixed continuously for 5 to 15 min, then spread on the wood and GFRP surfaces at a rate of 50 to 70 lb/ft^2. The 0.1875-in. by 4-in. by 20-ft GFRP plates were then bonded to the finished beams after an open assembly time of approximately 10 min at 70°F. A clamping pressure of 50 to 70 lb/in^2 was applied for 24 h to achieve curing of the adhesive, as recommended by the manufacturer. The wood beams had been finished to a 4-in. width after manufacture, and no additional surfacing was necessary after the bonding of the GFRP layers.

For the six beams with two layers of GFRP in the tension zone, a two-step process was used prior to the application of the clamping pressure. One GFRP layer was bonded to the glulam beam as previously described; then, the next GFRP layer was bonded with epoxy. The specified working time for this adhesive is 1 to 2 h at 75°F. After the first GFRP layer was bonded to the glulam beam, a thin layer of the epoxy was applied only to the second layer, which was placed on the already attached GFRP layer.

After curing, the 12 beams were inspected to verify that the GFRP surfaces were adequately bonded. We found one beam, with bottom reinforcement only, that had an inadequate bond between the wood and GFRP layers.

Evaluation Procedures

Finger-Jointed Lumber

The two groups of fabricated finger joints were tested to determine their ultimate tensile strength performance. The QC finger-joint specimens were tested in tension at the laminating plant following AITC Test T119 procedures (AITC 1992). The test finger-joint specimens were tested in tension in the laboratory following procedures given in ASTM D198 (ASTM 1992b). The primary difference between the two test procedures is that the AITC test targets a total time to failure of 3 to 5 min, whereas the ASTM test targets a total time to failure of approximately 10 min. Also, the QC finger-joint specimens were tested within 24 h of manufacture, whereas the laboratory-tested finger joints were tested after approximately 1 month. Data recorded for the AITC tests included width, thickness, ultimate load, total time to failure, percentage of finger-joint cross-section failure, percentage of wood failure in the end joint, and failure mode. In addition to these data, ASTM test data included transverse vibration MOE for the finger-jointed pieces of lumber and specific gravity specimens from the lumber on either side of the joint.

Glulam Beam

The 12 glulam-GFRP beams were tested in bending in accordance with ASTM D198 (ASTM 1992b). Of the 12 beams, 5 were tested with GFRP on the bottom, 6 with GFRP on top and bottom, and 1 without GFRP, because of the observed unsatisfactory bond obtained between the wood and GFRP.

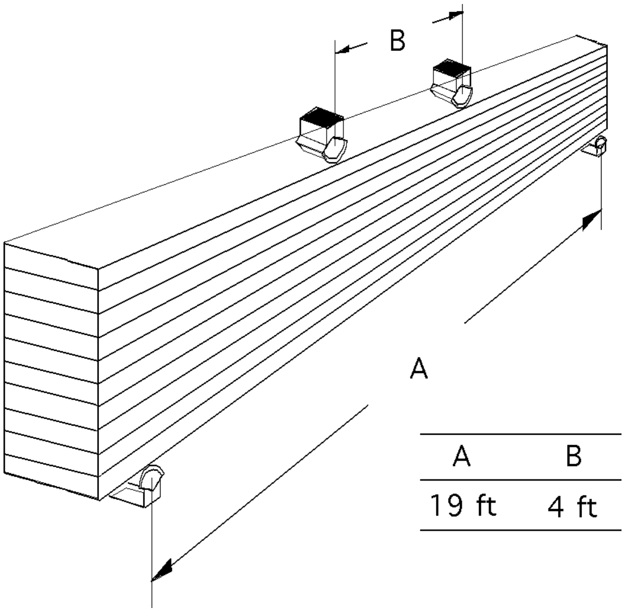

Figure 2—Loading configuration for bending tests of glulam beams.

The beams were tested under two-point loading with a load span of 4 ft and a support span of 19 ft (Fig. 2). Lateral bracing was provided at four locations along the length to prevent lateral-torsional instability of the beams. Midspan deflections were measured using a graduated ruler attached at mid-depth and a tensioned wire attached to the beam over each support. Additional deflections were recorded using linear variable differential transducers (LVDTs) positioned on the floor beneath midspan of the beam and under the load points. To verify the accuracy of the LVDT and the string line, dial gages were initially used to measure the deflection for a load up to 20 percent of the estimated ultimate load-carrying capacity of the beam.

Strains were recorded at various locations throughout the depth at midspan of each beam with four 2-in. strain gages, which were selected and bonded following recommendations given by Loferski and others (1989) and Yadama and others (1991). Location of the gages for each beam are listed in Table 5. Loads were measured with a load cell at the loading head. Readings from the LVDTs, strain gages, and load cell were recorded using a computerized data acquisition system.

Preliminary tests were conducted at a load of approximately 20 percent of the estimated ultimate load to provide data so that the linearity of the results could be evaluated. The final load test rate was adjusted to produce a failure in approximately 10 min per recommendation (ASTM 1992b). Strains and displacements were recorded up to ultimate load.

For the linear-response evaluation, a linear regression of the LVDT load–deflection data for up to half the failure load was used to determine the MOE for each beam. Modulus of rupture (MOR) was calculated using ultimate load and dimensions of the beam. Strain data were analyzed using a linear regression of the data up to half the failure load. Then, a best-fit linear strain gradient line was obtained from the four gages using a linear regression. This provided both a gradient and an estimate of the neutral axis location.

Table 5—Results of strain measurements on glulam beams taken at midspan

Beam	GFRP configuration	Gage 1 (bottom) slope [in/in·lb]	Gage 2 Location from bottom (in.)	Gage 2 Slope [in/in·lb]	Gage 3 Location from top (in.)	Gage 3 Slope [in/in·lb]	Gage 4 (top) Slope [in/in·lb]	Calculated neutral axis location from bottom (%)
3	none	0.185	3.250	0.075	2.950	–0.096	–0.178	48.2
1	2B	0.138	3.625	0.059	2.950	–0.099	–0.177	45.0
2	2B	0.148	3.625	0.071	2.950	–0.126	–0.149	46.9
5	2B	0.140	3.625	0.046	4.550	–0.063	—	44.4
6	2B	0.129	2.325	0.080	2.950	–0.090	–0.150	46.1
9	2B	0.137	2.325	0.093	2.950	–0.080	–0.157	48.2
4	T&B	0.146	2.138	0.104	2.138	–0.145	–0.188	44.0
7	T&B	0.150	3.438	0.081	3.138	—	–0.153	50.4
8	T&B	0.142	4.738	0.039	3.438	–0.076	–0.148	48.7
10	T&B	0.174	3.428	0.075	3.438	–0.073	–0.154	51.7
11	T&B	0.143	2.138	0.104	3.438	–0.066	–0.142	51.0
12	T&B	0.150	2.138	0.088	3.438	–0.057	–0.148	50.4

Table 6—Results of testing on the GFRP coupons

Property	Sample size	Average (lb/in²)	COV[a] (%)
Longitudinal tensile modulus	4	6.03×10^6	1.0
Poisson’s ratio	4	0.235	1.0
Tensile strength	10	130,000	1.7
In-plane shear modulus	5	687,000	2.9

[a]COV is coefficient of variation.

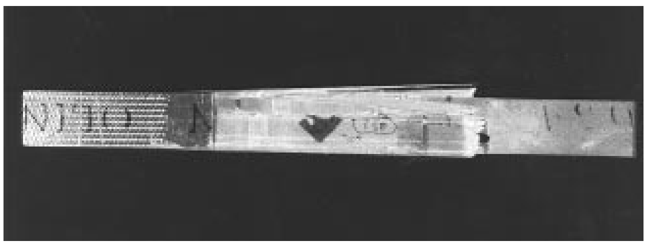

Figure 3—Tensile failure of GFRP coupon.

Results And Discussion

GFRP Evaluation

Results of testing on the GFRP coupons are given in Table 6. Tensile testing of the 0.75- by 0.1875- by 8.0-in. GFRP coupons (Fig. 3) resulted in an average tensile MOE of 6.025×10^6 lb/in^2, an average tensile strength of 130,000 lb/in^2, and a Poisson’s ratio of 0.235. Based on torsion tests, an average shear modulus of 687,000 lb/in^2 was obtained (Davalos and others 1996).

Lumber Evaluation

Results of the lumber properties used in the beams are given in Table 7. Note that the average MOE of the 2.0E grades is slightly less than the target range of 2.0 to 2.1×10^6 lb/in^2. However, this average value would meet the requirements for E-rated lumber given by AITC 117 Manufacturing (AITC 1993). Figure 4 illustrates the relationship between static and dynamic MOE for a representative group of No. 2 grade lumber that was tested. All lumber meeting the 2.0E–1/6 and 2.0E–1/3 grades was tested using a static deflection method. Note that the 10 No. 2 grade specimens tested for calibration resulted in an r^2 value of 0.96. Because the difference between static and dynamic MOE was small, the actual dynamic MOE values were used for the No. 2 grade of lumber, and data adjustments were not made.

Results of the knot properties for the 2.0E–1/6, 2.0E–1/3, and No. 2 grades are also included in Table 7. The knot sizes reported in Table 7 were compared with the results from a previous study (Moody and others 1993) for nominal 2- by 6-in. Yellow-Poplar. We observed that the average and maximum knot sizes from both studies were similar for the 2.0E–1/6, 2.0E–1/3, and No. 2 grades of Yellow-Poplar lumber.

Table 7—Results of lumber and knot properties used in beam manufacture.

Grade	Number of pieces	MOE: Avg. ($\times 10^6$ lb/in^2)	MOE: COV (%)	Knot properties: Length (ft)	Knot properties: $\bar{x}$[a] (%)	Knot properties: $\bar{x}$ + h[b] (%)
2.0E–1/6	61	1.94[c]	6.6	492	1.0	33.2
2.0E–1/3	69	1.95[c]	7.6	205	3.4	48.1
No. 2	65	1.63[d]	11.4	205	7.1	46.3

[a] $\bar{x}$ is the average of sum of all knot sizes within each 1-ft length, taken at 0.2-ft intervals expressed as a percentage of lumber width.
[b] $\bar{x}$ + h is equal to 99.5 percentile knot size (ASTM 1992a).
[c]Determined from static deflection tests.
[d]Determined from transverse vibration tests.

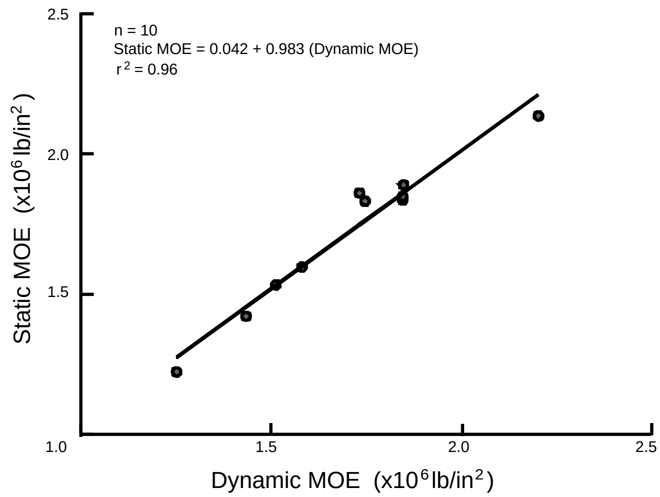

Figure 4—Relationship betwen dynamic and static MOE.

Finger-Jointed Lumber Evaluation

Results of QC and test finger-joint specimens are summarized in Table 8. Only those specimens that failed across the finger joint were considered in these summary statistics. Detailed information on the individual finger-joint test results is provided in Appendix A.

In comparing the results of the 2.0–1/6 end joints, we observed that the average tensile strength of 5,570 lb/in^2 of the QC specimens exceeded the 5,030 lb/in^2 level of the test specimens by approximately 10 percent. Also, the coefficient of variation (COV) in tensile strength for the test specimens (45.2 percent) was observed to be nearly three times that of the QC specimens (17.3 percent). Because the test specimens

Table 8—Results of finger-jointed lumber tests[a]

Finger-jointed lumber grade	Sample size	Cross section (in.) Width	Cross section (in.) Thickness	Ultimate tensile strength Average (lb/in^2)	COV (%)	5th percentile[c] (lb/in^2)
QC specimens meeting 2.0–1/6 criteria[b]	10	5.0	1.375	5,570	17.3	3,830
Test specimens meeting 2.0–1/6 grade criteria	31	4.0	1.300	5,030	45.2	2,053
2.0–1/6 test specimens meeting TL criteria	16	4.0	1.300	5,870	13.0	4,510
2.0–1/6 test specimens not meeting TL criteria	15	4.0	1.300	4,020	52.8	1,320
Test specimens meeting No. 2 grade criteria	28	4.0	1.300	4,530	39.7	2,040

[a]COV is coefficient of variation; QC is quality control; TL is special tension lamination.
[b]QC specimens were manufactured prior to glulam beam manufacture and tested in tension at the laminating plant following AITC T119 recommendations (AITC 1992); Test specimens were manufactured during glulam beam manufacture and tested in the laboratory in tension following ASTM D198 recommendations (ASTM 1992b).
[c]5th percentile is calculated at 75-percent tolerance.

Table 9—Bending stiffness and strength results of reinforced and unreinforced glulam beams

Reinforcement	Sample size	Cross section (in.) Width	Cross section (in.) Depth	MOE Average ($\times 10^6$ lb/in^2)	MOE COV[a] (%)	MOR Average (lb/in^2)	MOR COV (%)
None	1	4.0	13.0	1.86	—	6,000	—
Bottom only	5	4.0	13.375	2.00	1.4	9,010	6.9
Top and bottom	6	4.0	13.375	2.05	3.0	7,940	7.1

[a]COV is coefficient of variation.

were fabricated during the same production run as the test glulam beams, it is likely that the test glulam beams were manufactured with similar joints. Both groups of 2.0–1/6 finger joints in this study had average tensile strength values that were slightly less than the 5,830 lb/in^2 value observed by Moody and others (1993). They observed a COV in tensile strength for the 2.0–1/6 end joints of 24.9 percent.

Of particular interest concerning the test group of 2.0–1/6 finger joints is the average tensile strength of those specimens that met special tension lamination criteria. Table 8 shows that the average tensile strength of this group was 5,870 lb/in^2, with a COV of 13 percent. The performance level of this group would qualify these joints for glulam beams, targeting a design bending stress of 2,400 lb/in^2. In contrast, the 2.0–1/6 end joints that did not meet special tension lamination criteria performed at a tensile strength level that was less than the No. 2 grade specimens.

Glulam Beam Evaluation

Table 9 presents the average MOE and MOR data for the glulam beams. Results of the strain measurements are given in Table 5 and provide both a measure of the strain gradient and the location of the neutral axis. Appendix B provides detailed information on the individual beam MOE and MOR results and descriptions of the individual beam failures. Appendix C contains illustrations of the failure observed for each glulam beam test. Appendix D contains plots of the load–deflection and strain response curves for each of the beam tests.

Failure Response

Most beams failed catastrophically without significant visible failures before reaching ultimate load. Compression wrinkling was observed in the top wood laminations for three of the five beams with bottom reinforcement. For all beams, two events appeared to happen simultaneously at ultimate load. The most obvious was that the GFRP on the tension side delaminated completely from the adjacent wood tension lamination. The second event, obvious upon inspection of the beams, was that the failure occurred through a finger joint in the outermost wood lamination on the tension side. Based on observations during tests and the post-failure examination, all failures were believed to have initiated at finger joints in the bottom (tension) wood layers near midspan of the beam.

The delamination of the GFRP composite layer from the wood occurred, in most cases, with essentially no wood failure; no trace of wood was observed in the delaminated GFRP panel. There was no obvious damage to the composite nor did there appear to be any significant problem with the epoxy bond between the two layers of GFRP for the five beams with bottom reinforcement only. The delamination was not consistent with the results of prior research in which adequate bonding was obtained using the same adhesive (Munipalle 1992). Several differences were noted between the conditions of the previous research and those used to manufacture beams in our study. The GFRP was somewhat higher in density of the fiber content (60 percent by volume), and a resin-rich layer was present on the bonding surface that could not be efficiently etched by sanding (i.e., inadequate surface texture). Other possible differences (but not likely) include inappropriate curing time and temperature for the adhesive. This bonding problem indicates that additional research is necessary to produce adequate interlaminar bond strength between wood and GFRP under plant conditions.

Stiffness Performance

As shown in Table 9, the MOE for the two beam combinations averaged 2.00×10^6 lb/in^2 for beams with two GFRP layers on the bottom and 2.05×10^6 lb/in^2 for beams with one GFRP layer each on the top and bottom. Thus, the average MOE of the six beams with top and bottom reinforcement was about 3 percent greater than that of the five beams with bottom reinforcement only. Although statistical significance could not be proved based on the small sample sizes tested, the results correspond to the 1.4-percent difference predicted in Table 3 using design lumber MOE properties.

In addition to determining glulam MOE from full-span load–deflection measurements, the distribution of stresses was also evaluated by monitoring the strain responses across the beam depths. Table 5 summarizes the calculated slopes of the strain measurements (Appendix D) for various locations along the depth for each of the 12 beams that were tested. Based on the experimentally measured strain distributions, the location of the neutral axis was determined for each beam and are given in Table 5.

The MOE values of the beam depend directly on the MOE properties of the component GFRP and lumber. A comparison of the assumed (Table 2) and actual MOE values (Tables 6 and 7) of the lumber indicate little difference. The actual MOE of the 2.0E lumber was slightly less than that assumed, and the MOE for the No. 2 grade lumber was slightly greater than assumed. Based on the observed properties of the lumber, predicted glulam MOE using ASTM D3737 procedures and actual lumber properties was 2.08×10^6 lb/in^2 for the beam combination with two GFRP layers on the bottom and 2.11×10^6 lb/in^2 for the beam combination with one GFRP layer each on the top and bottom (Table 10). The predicted MOE of the beams using actual lumber MOE properties with top and bottom reinforcement was 2 percent greater than that of the beams with bottom reinforcement only. Predicted results were 3 to 4 percent greater than actual results for both combinations.

To determine the percentage increase in glulam MOE as a result of the influence of the GFRP layers using actual lumber properties, ASTM D3737 procedures were used to predict the MOE of a beam without the GFRP laminations. A direct comparison was conducted by replacing the GFRP layers with an equal depth of lumber. Based on this analysis method, increases in MOE of 16 and 18 percent were predicted for the combinations shown in Figure 1 (Table 10).

Strength Performance

In Table 9, the actual glulam MOR results for the two beam combinations were found to be 9,010 lb/in^2 for the five beams with two GFRP on the bottom and 7,940 lb/in^2 for the six beams with one GFRP layer each on the top and bottom. Thus, the beams with bottom reinforcement only averaged 13 percent greater in bending strength than beams with top and bottom reinforcement. Again, statistical significance was not determined due to the small sample sizes; however, results corresponded to those predicted in Table 3.

To qualitatively discuss possible failure mechanisms, a linear load–deflection response was assumed for the glulam beams. This assumption is accurate, as illustrated in Appendix D, for beams with a balanced layup. However, for beams with GFRP reinforcement on the bottom only, nonlinearities were observed in the strain response of the compression wood layers, also illustrated in Appendix D. Given the assumed linear response behavior, the bending strength of the combinations was predicted using ASTM D3737 procedures for all-wood glulam beams and using actual GFRP and lumber properties from Tables 6 and 7, respectively. A ratio of 2.898 was used to calculate an average bending strength from the calculated design bending strength, which was observed by Moody and others (1993) for Yellow-Poplar glulam. To adjust the calculated average bending strength to a strength corresponding to a standard size beam, a volume effect adjustment of 1.021 was applied. This adjustment is based on the volume effect equation specified by AITC (1991) and the volume effect exponent of 0.088 observed by Moody and others (1993) for Yellow-Poplar glulam.

Table 10—Glulam beam MOE and MOR predicted with ASTM D3737 procedures (ASTM 1992a)[a]

GFRP configuration	Actual with GFRP (1)	Predicted with GFRP (2)	Predicted without GFRP (3)	Prediction ratio (2) ÷ (1)	Predicted increase (2) ÷ (3)
Average MOE ($\times 10^6$ lb/in^2)					
2 bottom	2.00	2.08	1.79	1.04	1.16
1 top, 1 bottom	2.05	2.11	1.79	1.03	1.18
Average MOR (lb/in^2)					
2 bottom	9,010	8,640	6,880	0.96	1.26
1 top, 1 bottom	7,940	7,780	6,620	0.98	1.18

[a]ASTM D3737 provides predictions for glulam beam MOE and design bending stress. Design bending stress was converted to average glulam MOR by multiplying by the ratios 2.898 and 1.021. The 2.898 ratio is the relationship observed between average glulam MOR and design bending stress for Yellow-Poplar (Moody and others 1993). The 1.021 ratio is the volume effect adjustment based on a volume effect exponent of 0.088 (Moody and others 1993).

The results in Table 10 show that the predicted average MOR for glulam beams with bottom reinforcement was 8,640 lb/in^2, and that for beams with top and bottom reinforcement was 7,780 lb/in^2. Both predicted values are within 5 percent of the actual test values. To determine the increase in average bending strength as a result of the presence of the GFRP layers, ASTM D3737 procedures were used to predict the performance of a glulam beam without reinforcement. Similar to the MOE comparison, a direct comparison was conducted by replacing the thin GFRP layers with an equal depth of lumber. The predicted average MOR for the simulated nonreinforced glulam beam (bottom) combination with wood only added on the bottom was 6,880 lb/in^2. For the simulated glulam combination with the thin layers of wood applied to both the top and bottom, the predicted average MOR was 6,620 lb/in^2. Using these values as the basis for comparison, the predicted increase in average MOR was 26 percent for the beams with reinforcement on the bottom and 18 percent for the beams with reinforcement on both the top and bottom. In our study, the strength predictions with ASTM D3737 compared well with experimental results. However, to predict the progression of localized failures and the complex distribution of stresses as a result of using two materials with significantly different MOE values, a more sophisticated modeling procedure would be necessary (Davalos and others 1996, Kim and others 1996).

Strain Response

Based on the failure maps and the actual properties of the lumber (Appendix C), the tensile and compressive ultimate stresses at critical locations of the beams were calculated. For beams with GFRP reinforcement on both the top and bottom, the average calculated stresses at the outermost wood laminations were 7,530 lb/in^2 (6.4 percent COV) on the tension side and 7,500 lb/in^2 (6.4 percent COV) on the compression side. For beams with GFRP reinforcement on the bottom only, the average calculated stresses at the outermost wood laminations were 7,250 lb/in^2 (19.1 percent COV) on the tension side and 9,350 lb/in^2 (7.7 percent COV) on the compression side. Based on this analysis, it is apparent that the stresses at failure are approximately equal on the tension and compression wood layers for beams with top and bottom reinforcement. The tensile and compressive strength of lumber is approximately equal for higher quality grades (Green and Evans 1987). Therefore, you would expect these beams to fail because of tension failures and compression wrinkling in about equal proportions if finger joints were not part of the assembly. However, because the finger-jointed lumber in this study was lower in tensile strength than the solid lumber, failure would probably occur on the tension side at a finger-joint location.

For beams with reinforcement on the bottom only, the ratio between the calculated compression stress to the calculated tension stress was 1.29, as a result of the downward shift of the neutral axis. For these beams, failure stresses in compression would be the first to be reached. If the tensile strength of the finger joints does not meet a level that is approximately 77 percent (inverse of the ratio 1.29) of the compressive strength of the lumber, the beams would then likely fail in tension at a finger joint. Given the less than expected finger-joint results shown in Table 8 and the fact that all beams had failures associated with a finger joint, this analysis indicates that finger-joint strength was the controlling factor for the glulam beams in our study. It is likely that improved finger joints in the beams with two GFRP layers on the tension side would have resulted in more beams having a principal mode of failure on the compression side.

A similar comparative analysis was conducted for ultimate shear stress. Ultimate shear stress at the wood-GFRP interfaces and at the neutral axes was calculated for each beam. The computed shear stress values at the interfaces are significantly smaller than the average shear strength of approximately 1,280 lb/in^2 for the Yellow-Poplar/GFRP interface reported previously (Gardner and others 1994, Barbero and others 1994). Thus, the delamination of the GFRP reinforcement observed in the present study occurred under relatively small shear stresses, partly as a result of the high density and smooth surface texture of the composite. The shear stress, just prior to failure, at the neutral axes of the beams was quite low in relation to the shear strength of the approximately 1,800 lb/in^2 reported for Yellow-Poplar shear-block tests by Janowiak and others (1992).

Discussion of Alternative Design Approaches

Figure 5a illustrates the transformed section analysis method used by the ASTM D3737 procedure for calculating stress of glulam timber reinforced with a high strength, high stiffness composite on the bottom tension lamination. Basically, all laminations and their properties in the glulam beam are considered when calculating stress. Properties are based on bending stress indices and calculated strength ratios. Two additional methods that warrant consideration include (1) a modified ASTM D3737 procedure also based on bending stress indices and strength ratios, where only the compression-side wood laminations and the tension-side reinforcement are considered (Fig. 5b) and (2) a transformed section analysis similar to that used in reinforced-concrete design (Fig. 5c), which is based on allowable strength properties. However, note that the "compression stress block" used in the exploratory analysis of Figure 5c is assumed to have the same neutral axis as that used in Figure 5a,b. In actual reinforced-concrete analysis, the depth of the compression stress block is calculated so that the rectangular compression stress block has equal area and a corresponding centroid as the actual (nonlinear) stress block. In addition, the method shown in Figure 5c is based on allowable compression parallel-to-grain properties for the wood laminations, rather than bending stress indices and strength ratios.

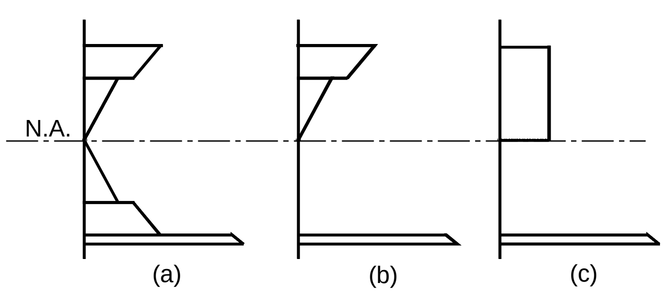

Figure 5—Possible design approaches for glulam beams reinforced with a high strength composite tension lamination: (a) ASTM D3737 method, (b) modified ASTM D3737 method, and (c) compression-block method.

An investigation was conducted to determine which method would provide the best results for predicting the performance of reinforced glulam beams. This investigation considered only the bending strength of beams reinforced on the bottom tension laminations, because this would be the most common application of composite reinforcement. The experimentally determined average MOR of 9,010 lb/in^2 was within 5 percent of the 8,640 lb/in^2 value predicted with the method shown in Figure 5a. This method predicted that failure would initiate in the first No. 2 grade lamination (third tension lamination). However, the low strength finger joints caused the initiation of beam failure to occur at the first tension lamination. Again, average MOR values were determined by multiplying the calculated design bending strength by 2.898 and 1.021 to adjust to an average bending strength of a standard size beam (design value-to-average-value adjustment), as discussed previously.

For the method illustrated in Figure 5b, the same ASTM D3737 analysis was carried out except that only the compression-side laminations and the high strength reinforcement were considered. (Wood tension laminations were ignored.) Also, ASTM D3737 suggests a compression bonus factor of 1.3 for adjusting compression-side bending stresses to predict compression failures in glulam beams. The calculated neutral axis was based on the MOE properties for all laminations. Based on this method, an estimated average MOR of 8,850 lb/in^2 was obtained, which is within 2 percent of the actual average MOR. This method ignores any failure in the wood tension laminations (solid or finger-jointed), always predicts a compression failure as a result of the high strength of the composite reinforcement, and assumes adequate bonding between the wood and GFRP layers. The same design-value-to-average-value adjustment was used.

For the compression-block method illustrated in Figure 5c, compression parallel-to-grain properties were assumed for the 2.0E–1/3 and No. 2 lumber grades based on values published in the National Design Specifications (NFPA 1991) for SS and No. 2 grades, respectively. Allowable compression parallel-to-grain stresses assumed for the 2.0E–1/3 grade and No. 2 grades were 900 lb/in^2 and 575 lb/in^2, respectively. Based on the same transformed section method as the previous two methods, an allowable resisting moment and a maximum allowable bending stress were obtained. Using the same design value-to-average-value adjustment factors, the average MOR based on the calculated allowable bending stress was 7,650 lb/in^2, which is within 18 percent of the actual average MOR.

In our investigation, simplified methods of analysis were compared to determine which method best predicted the performance of reinforced glulam beams. We found that all three methods could conservatively predict bending strength to within 20 percent of the actual results. In all methods, input properties of the laminations were based on assumed values. For the two ASTM D3737 methods, bending stress indices were based on values established in the ASTM D3737 standard for E-rated softwood species of lumber and on a factor of 1.3 for predicting compression failures in glulam. For the compression-block method, compression parallel-to-grain stresses were assumed based on published design values. However, note that these simplified analyses assume linear behavior up to ultimate failure and that not all failure modes (compression or tension side) could be reliably predicted by any one method. Future investigation of these simplified analysis methods is desirable.

Conclusions

The following conclusions and recommendations are presented regarding the reinforcement of glulam timber with E-glass fiber-reinforced plastic (GFRP):

- Given adequate bonding between GFRP and wood, GFRP offers the potential to improve the bending strength and stiffness performance of glulam beams.

- Although sample sizes were too small to warrant statistical significance, results indicate that adding 3 percent of GFRP by volume could increase bending stiffness by as much as 18 percent and bending strength by as much as 26 percent.

- Analysis methods suggest that adding reinforcement to the bottom tension laminations most efficiently improves beam bending strength. Similarly, analysis methods suggest that adding equal reinforcement to the top and bottom laminations most efficiently improves beam bending stiffness. However, the improved efficiency of top and bottom reinforcement is probably not significant enough to offset the added material and handling costs of two layers of GFRP.

- Comparisons of displacement and strain measurements indicate that the response of the glulam timber beams with one layer of GFRP on the top and bottom was nearly linear to failure and the stress conditions could be accurately predicted using basic mechanics. The strain response of the glulam beams with two GFRP layers on the bottom was slightly nonlinear at failure; however, predictions using basic mechanics were found to be acceptable. The strength of most beams was controlled by the tensile strength of the finger joints in the layer of wood adjacent to the GFRP. Improved joints would probably increase the strength of the beams with GFRP on both the tension and compression sides. However, for beams with GFRP on only the tension side, improved joints may shift the failure mode in the beams to the compression side, with possibly a slight increase in strength. With some modifications, ASTM D3737 procedures appear to be applicable for predicting the properties of the GFRP-glulam beams that show little to no sign of nonlinear strain response.

Literature Cited

AITC. 1991. Use of a volume effect factor in the design of glued laminated timber beams. Tech. Note 21. Vancouver, WA: American Institute of Timber Construction. October.

AITC. 1992. Inspection manual for structural glued laminated timber. AITC 200. Englewood, CO: American Institute of Timber Construction.

AITC. 1993. Standard specifications for structural glued laminated timber of softwood species. AITC 117. Englewood, CO: American Institute of Timber Construction.

AITC. 1996. Standard specifications for structural glued-laminated timber of hardwood species. AITC 119. Englewood, CO: American Institute of Timber Construction.

ANSI. 1992. ANSI/AITC A190.1. American Institute of Timber Construction. Englewood, CO: American National Standard Institute.

ASTM. 1992a. Standard method for establishing stresses for structural glued-laminated timber (glulam). ASTM D3737–91. Philadelphia, PA: American Society for Testing and Materials.

ASTM. 1992b. Standard methods for static tests of timber in structural sizes. ASTM D198–84. Philadelphia, PA: American Society for Testing and Materials.

Barbero, E.J.; Davalos, J.F.; Munipalle, U. 1994. Bond strength of FRP-wood interface. Journal of Reinforced Plastics and Composites. 13(9): 835–854.

Curtis, J.O. 1972. Steel reinforced wooden beams. Transactions of the American Society of Agricultural Engineers: 552–555.

Davalos, J.F.; Kim, Y.; 1996. A material degradation approach for failure prediction of ACM-reinforced glulam beams. In: Advanced composite materials in bridges and structures: 2nd international conference, CSCE, Montreal, Quebec, Canada: 803–810.

Davalos, J.F.; Salim, H.A.; Schlussel, J. 1996. Shear stiffness of pultruded FRP from torsion tests. In: Proceedings, 1st international conference on composites in infrastructure, ICCI '96, University of Arizona, Tucson, Arizona: 689–698.

Freas, A.D.; Selbo, M.L. 1954. Fabrication and design of glued laminated wood structural members. Tech. Bull. 1069. U.S. Department of Agriculture. Available from American Institute of Timber Construction, Englewood, CO.

Gardner, D.J.; Davalos, J.F.; Munipalle, U. 1994. Adhesive bonding of pultruded fiber-reinforced plastic (FRP) to wood. Forest Products Journal. 44(5): 62–66.

Green, D.W.; Evans, J.W. 1987. Mechanical properties of visually graded lumber: Volume 1, A summary. Available from National Technical Information Service, 5285 Port Royal Rd., Springfield, VA 22161.

Janowiak, J.J.; Manbeck, H.B.; Blankenhorn, P.R.; Kessler, K.R. 1992. Strength properties of exterior adhesives on preservative treated hardwoods. Forest Products Journal. 42(10): 68–76.

Kim, Y.; Davalos, J.F.; Barbero, E.J. 1996. Progressive failure analysis of laminated composite beams. Journal of Composite Materials. 30(5): 536–560.

Krueger, G.P.; Sandberg, L.B. 1974. Ultimate strength design of reinforced timber. Wood Science. 6(4): 316 –330.

Lantos, G. 1970. The flexural behavior of steel reinforced laminated timber beams. Wood Science. 2(3): 136–143.

Leichti, R.J.; Gilham, P.C.; Tingley, D.A. 1993. The Taylor Lake Bridge: A reinforced-glulam structure. Wood Design Focus. Summer.

Loferski, J.R.; Davalos, J.F.; Yadama, V. 1989. A laboratory-built clip-on strain gage transducer for testing wood. Forest Products Journal. 39(9): 45–48.

Mark, R. 1961. Wood-aluminum beams within and beyond the elastic range. Forest Products Journal. 11(10): 477–484.

Moody, R.C.; Hernandez, R.; Davalos, J.F.; Sonti, S.S. 1993. Yellow Poplar glulam timber beam performance. Res. Pap. FPL–RP–520. Madison, WI: U.S. Department of Agriculture, Forest Service, Forest Products Laboratory. 28 p.

Munipalle, U. 1992. Analysis and testing of wood-glass fiber reinforced plastic adhesive interface. Morgantown, WV: West Virginia University. M.S. thesis.

NELMA. 1991. Grading rules for northeastern lumber. Cumberland Center, ME: NorthEastern Lumber Manufacturers Association.

NFPA. 1991. National design specification for structural wood. Washington, DC: National Forest Products Association.

Peterson, J.L. 1965. Wood beams prestressed with bonded tension elements. American Society of Civil Engineers. Journal of the Structural Division. 91(1): 103–119.

Plevris, N.; Triantafillou, T.C. 1992. GFRP–reinforced wood as structural material. American Society of Civil Engineers. Journal of Materials in Civil Engineering. 4(3): 300–317.

Ross, R.J.; Geske, E.A.; Larson, G.H.; Murphy, J.F. 1991. Transverse vibration nondestructive testing using a personal computer. Res. Pap. FPL–RP–502. Madison, WI: U.S. Department of Agriculture, Forest Service, Forest Products Laboratory.

Spaun, F.D. 1981. Reinforcement of wood with fiberglass. Forest Products Journal. 31(4): 26–33.

Theakston, F.H. 1965. A feasibility study for strengthening timber beams with fiberglass. Canadian Agriculture Engineering. January: 17–19.

Tingley, D.A. 1994. Aligned fiber reinforcement panel for structural wood members. U.S. patent 5,362,545.

Triantofillou, T.C.; Deskovic, N. 1992. Prestressed GFRP sheets as external reinforcement of wood members. American Society of Civil Engineers. Journal of Structural Engineering. 118 (5): 1270–1284.

Western Wood Structures. 1994. High strength fiber reinforced plastic (FiRP) glulam. Brochure. Tualatin, OR: Western Wood Structures, Inc.

Yadama, V.; Davalos, J.F.; Loferski, J.R.; Holzer, S.M. 1991. Selecting a gage-length to measure parallel-to-grain strain in southern pine. Forest Products Journal. 41(10): 65–68.

Appendix A—Finger-Joint Evaluation

Table A1 contains results of all finger-joint tests, including those of specimens that did not fail at the joint.

Table A1—Finger joint evaluation[a]

Side A ID no.	Side-B ID no.	Lum-ber grade	MOE ($\times 10^6$ lb/in^2)	Max stress (lb/in^2)	MC A (%)	MC B (%)	SG A	SG B	TTF (M:S)	Fail X-sect (%)	Wood of fail (%)	AITC failure type	Failure zone (A to B)	Notes
Quality Control specimens tested at the laminating plant														
10	11	1A		4418					0:35	100	0			
6	5	1A		3826					0:35	100	0			
7	6	1A		6489					1:20	50	50			
8	7	1A		5158					1:35	80	20			
12	11	1A		5750					1:30	97	3			
9	8	1A		5750					1:20	15	85			
1	2	1A		6637					1:40	90	10			
2	3	1A		5897					1:30	75	25			
3	4	1A		5602					1:45	40	60			
9	10	1A		6045					1:20	100	100			
4	5	1A	Saved for delamination test											
Test specimens tested in the laboratory														
64	85	1A	1.83	6685	8.7	6.7	0.57	0.51	6:50	20	100	5	0,0	
125	189	1A	2.05	5454	9.4	9.5	0.53	0.57	5:34	10	25	5	-10,+12	
171	6	1A	1.72	6085	8.2	9.1	0.51	0.47	6:10	25	50	5	-8,+8	
175	168	1A	1.63	6904	8.9	8.2	0.49	0.45	7:04	100	100	2	0,0	
180	149	1A	1.61	4877	9.8	9.1	0.51	0.49	4:58	1	0	5	0,+10	
187	124	1A	1.75	5388	9.5	9.6	0.51	0.48	5:31	80	100	4	0,+6	
243	642	1A	2.00	5592	9.2	8.3	0.49	0.46	5;42	100	80	2	0,0	
430	426	1A	2.00	6615	10.2	9.3	0.51	0.52	6:42	1	0	5	-14,0	
431	554	1A	1.87	5892	8.4	9.7	0.53	0.51	6:00	100	90	3	0,0	
500	508	1A	2.07	6642	9.3	9.6	0.50	0.49	6:47	100	0	1	0,0	
532	535	1A	1.84	5327	9.6	8.1	0.45	0.45	5:25	100	20	1	0,0	
628	278	1A	1.71	4692	8.9	9.3	0.46	0.46	4:46	1	0	5	-20,0	
629	24	1A	2.12	6877	9.4	9.8	0.49	0.48	6:56	100	100	2	0,0	
629	630	1A	1.93	4858	11.0	9.3	0.46	0.47	4:56	1	0	5	-36,0	at 20% CK+GD
636	243	1A	1.71	6342	9.3	9.4	0.49	0.55	6:26	1	0	5	0,+18	
1028	1027	1A	1.97	5581	8.9	8.6	0.52	0.51	5:41	100	0	1	0,0	
20	200	1B	1.81	4292	9.7	9.4	0.40	0.46	4:20	1	0	5	-12,+0	
87	426	1B	1.96	4108	8.4	10.1	0.60	0.57	4:11	15	100	5	-4,0	
92	630	1B	1.75	6492	9.4	10.2	0.47	0.46	6:36	95	90	2	0,0	
92	580	1B	1.90	6627	8.7	9.2	0.58	0.56	6:44	90	75	2	-2,+0	
112	64	1B	1.77	4204	7.9	8.0	0.49	0.56	4:16	10	100	5	0,+3	
141	145	1B	1.96	1662	9.2	9.5	0.56	0.52	1:43	100	15	1	0,0	
163	105	1B	1.70	1500	9.2	9.6	0.49	0.58	1:32	100	60	1	0,0	
191	141	1B	1.71	1554	10.0	10.2	0.48	0.55	1:36	100	25	1	0,0	
344	337	1B	1.78	3323	9.6	9.8	0.59	0.52	3:22	20	75	5	-10,+0	
532	543	1B	1.88	3015	9.5	9.2	0.48	0.50	6:59	33	0	5	-20,+40	
624	600	1B	1.92	6408	10.8	8.7	0.46	0.55	6:29	20	100	5	+3,+5	
628	627	1B	2.03	2892	10.0	7.6	0.60	0.58	2:55	85	95	2	0,+14	
1053	1052	1B	1.88	3485	9.8	9.1	0.47	0.49	3:24	30	25	5	0,+10	
1086	1087	1B	1.96	4900	9.2	8.9	0.51	0.48	4:58	1	0	5	0,+24	
2066	2065	1B	1.84	4719	9.7	9.3	0.51	0.57	4:49	1	0	5	+1,+8	
61	430	2	1.41	6473	9.3	10.5	0.59	0.64	6:36	100	30	1	0,0	
66	83	2	1.30	3819	9.9	8.2	0.55	0.44	3:53	50	80	5	0,+8	
81	101	2	2.06	5362	9.6	9.1	0.59	0.55	5:29	95	60	1	0,0	
96	157	2	1.59	2758	8.8	8.9	0.45	0.50	2:49	1	0	5	0,+40	
102	130	2	1.79	4377	9.3	10.9	0.55	0.46	4:27	25	50	5	0,+5	at 30% EK+GD

Table A1—Finger joint evaluation—con.

Side A ID no.	Side-B ID no.	Lumber grade	MOE ($\times10^6$ lb/in^2)	Max stress (lb/in^2)	MC A (%)	MC B (%)	SG A	SG B	TTF (M:S)	Fail X-sect (%)	Wood of fail (%)	AITC failure type	Failure zone (A to B)	Notes
105	123	2	1.62	4165	8.8	9.3	0.52	0.47	4:16	40	100	5	-20,+5	
119	191	2	1.18	1596	9.5	7.1	0.41	0.34	1:39	1	0	5	-7,0	
130	158	2	1.60	4073	10.7	9.5	0.48	0.41	4:09	100	95	4	0,0	
144	122	2	1.53	4423	8.6	10.0	0.45	0.39	4:33	20	100	5	0,+5	
167	188	2	1.12	1450	9.3	8.8	0.35	0.56	1:29	100	70	3	-4,0	
168	105	2	1.58	5942	9.5	8.9	0.41	0.54	6:03	100	60	1	0,0	
196	186	2	1.48	3831	10.8	9.7	0.41	0.53	3:55	70	90	3	0,0	
344	342	2	1.46	3165	9.6	9.9	0.49	0.42	3:12	50	50	5	-10,0	
352	346	2	1.82	3250	9.6	9.6	0.51	0.48	3:19	1	0	5	0,+12	
620	276	2	1.42	5662	8.4	9.8	0.40	0.40	5:45	5	40	5	0,0	
639	247	2	1.56	6042	9.0	10.2	0.47	0.54	6:09	100	25	1	0,0	
642	246	2	1.51	5696	9.4	9.1	0.76	0.52	5:46	100	50	1	0,0	
1002	1001	2	1.69	6740	9.4	8.6	0.42	0.48	6:55	100	85	2	0,0	
1006	1005	2	1.55	5215	8.0	9.2	0.49	0.45	5:19	100	100	4	0,+8	
1008	1007	2	1.64	7008	10.3	9.8	0.53	0.46	7:09	15	75	5	-8,+0	
1011	1010	2	1.95	6096	9.4	9.8	0.52	0.56	6:12	20	50	5	0,+30	
1019	1018	2	1.56	3396	9.1	7.8	0.39	0.46	3:26	5	50	5	-12,0	
1026	1025	2	1.45	4512	9.8	8.5	0.51	0.51	4:36	25	50	5	-4,+8	
1035	295	2	1.28	3942	10.2	9.7	0.40	0.52	4:33	15	100	5	0,+15	
1050	1051	2	1.45	2950	8.1	9.8	0.58	0.43	3:00	80	0	4	0,0	
1061	1060	2	1.51	4446	9.8	8.9	0.43	0.42	4:31	5	100	5	0,+20	
1063	1062	2	1.47	4365	9.5	9.2	0.47	0.44	4:27	30	100	5	0,+10	
1066	1065	2	1.62	4500	9.1	9.5	0.48	0.53	4:35	1	0	5	-6,+6	
Test specimens that did not fail at finger joint														
508	431	1A	2.16	6408	9.9	9.1	0.53	0.52	6:31	0	0	6	+15,+17	at 40% CK+GD
624	625	1A	1.82	6931	9.1	9.4	0.44	0.47	7:00	0	0	6	+5,+8	at 25% CK+GD
1013	1012	1A	1.67	4965	8.4	9.5	0.47	0.45	5:04	0	0	6	-24	
1084	1085	1A	1.68	4377	9.7	8.7	0.49	0.38	4:28	0	0	6	+20,+22	at 20% CK+GD
627	125	1B	1.85	4700	9.1	10.3	0.50	0.48	4:47	0	0	6	-12,-15	
32	235	2	2.01	6712	9.4	7.8	0.50	0.44	6:51	0	0	6	-20,-18	at 30% CK+GD
61	200	2	1.51	4892	9.5	7.6	0.57	0.48	4:58	0	0	6	-4	at 15% CK+GD
100	1090	2	1.33	1896	11.1	9.2	0.47	0.45	1:58	0	0	6	-35,-30	at 40% EK+GD
103	116	2	1.51	1477	8.3	9.4	0.51	0.58	1:34	0	0	6	+54,+56	at 60% EK+GD
108	186	2	1.46	2446	9.6	8.9	0.49	0.43	2:30	0	0	6	+14,+20	at 40% EK+GD
117	124	2	1.57	3508	8.5	8.4	0.50	0.41	3:35	0	0	6	+36,+42	at 5% CK+GD
118	180	2	1.37	3231	10.3	10.7	0.52	0.52	3:18	0	0	6	+3,+8	
119	176	2	1.39	2815	9.6	9.0	0.45	0.52	2:51	0	0	6	+28,+42	
122	96	2	1.29	1450	8.9	9.4	0.40	0.49	1:30	0	0	6	-25,-15	
136	191	2	1.60	3012	9.3	8.7	0.55	0.35	3:03	0	0	6	-44,-42	
145	190	2	1.68	1569	9.4	8.3	0.47	0.59	1:36	0	0	6	+5,+24	at 55% EK+GD
155	186	2	1.42	2523	8.3	9.5	0.42	0.43	2:35	0	0	6	+4,+8	
159	123	2	1.37	2027	8.6	11.3	0.46	0.47	2:04	0	0	6	-48,-45	
177	1092	2	1.47	8215	9.3	9.0	0.54	0.51	8:24	0	0	6	-12,-6	
182	197	2	1.45	4742	8.7	9.0	0.42	0.48	4:50	0	0	6	+12,+14	
189	112	2	1.68	3450	9.6	8.4	0.57	0.49	3:29	0	0	6	-8	at 40% EK+GD

Table A1—Finger joint evaluation—con.

Side A ID no.	Side-B ID no.	Lumber grade	MOE ($\times 10^6$ lb/in^2)	Max stress (lb/in^2)	MC A (%)	MC B (%)	SG A	SG B	TTF (M:S)	Fail X-sect (%)	Wood of fail (%)	AITC failure type	Failure zone (A to B)	Notes
192	247	2	1.67	5565	8.8	9.2	0.45	0.50	5:37	0	0	6	+10,+12	at 40% CK+GD
251	252	2	1.13	2292	8.7	9.1	0.50	0.31	2:18	0	0	6	-12,-10	at 40% GD
310	302	2	1.47	3704	7.4	9.9	0.57	0.45	3:46	0	0	6	+12,+20	at 1:6 SOG
314	310	2	1.41	1927	9.6	12.9	0.54	0.55	1:58	0	0	6	-7,+5	
317	337	2	1.41	1788	8.8	9.2	0.51	0.47	1;49	0	0	6	-9,-3	
335	312	2	1.62	4208	10.1	9.1	0.52	0.49	4:20	0	0	6	+20,+24	at 80% EK+GD
341	335	2	1.57	2481	10.5	10.0	0.48	0.61	2:31	0	0	6	+14,+20	at 1:8 SOG
342	352	2	1.67	3573	9.7	9.8	0.44	0.49	3:33	0	0	6	-17,-7	
346	336	2	1.82	3492	9.8	9.7	0.51	0.56	3:34	0	0	6	18,+24	
357	356	2	1.50	2846	10.1	10.1	0.47	0.47	3:29	0	0	6	+25,+30	
543	554	2	1.33	1754	9.0	8.8	0.48	0.53	1:48	0	0	6	+3,+8	at 85% GD
639	620	2	1.81	5765	8.5	8.5	0.46	0.46	6:08	0	0	6	+7,+9	
1004	4003	2	1.52	4054	9.2	8.5	0.41	0.41	4:05	0	0	6	-6,-12	
1015	1014	2	1.36	2419	9.1	9.2	0.48	0.53	2:28	0	0	6	-24,-26	at 30% EK+GD
1017	1016	2	1.37	1842	9.2	9.6	0.41	0.47	^1:51	0	0	6	+10,+30	at 1:6 SOG
1021	1020	2	1.39	2796	9.2	7.8	0.43	0.47	3:24	0	0	6	-18,-25	at 40% EK+GD
1029	1030	2	1.39	1600	9.2	10.3	0.57	0.48	1:37	0	0	6	-12,-8	at 50% EK+GD
1031	1032	2	1.44	4442	9.4	8.7	0.51	0.38	2:22	0	0	6	+24	at 60% CK+GD
1034	1033	2	1.55	3015	10.0	8.7	0.38	0.45	3:06	0	0	6	-20,-30	
1038	1039	2	1.34	1642	8.8	8.6	0.46	0.46	1:40	0	0	6	-22,+2	
1043	1042	2	1.60	4523	8.4	8.3	0.48	0.51	4:34	0	0	6	-28,-24	
1055	1054	2	1.58	4442	8.8	7.3	0.48	0.42	4:32	0	0	6	+2,+6	at 35% EK+GD
1057	1056	2	1.46	2200	8.5	10.1	0.49	0.43	2:09	0	0	6	+10,+14	
1080	1081	2	1.76	4277	8.4	7.8	0.46	0.47	4:21	0	0	6	+30,+35	at 50% CK+GD
1082	1083	2	1.65	3269	9.6	10.0	0.42	0.41	3:13	0	0	6	+20,+30	at 50% EK+GD

[a]**Lumber Grade:** 1A = 2.0-1/6 grade that meets tension lamination criteria; 1B = 2.0-1/6 grade that does not meet tension lamination criteria; 2 = No. 2 grade

MOE is the modulus of elasticity of the finger-jointed specimen determined using a transverse vibration test.

Max stress is the maximum tensile stress determined using the load at failure and cross-sectional dimensions measured prior to test.

MC A and **B** are moisture content measured from test blocks using an ovendry method. Test blocks were cut from the failed specimen.

SG A and **B** are specific gravity determined from the same moisture content test blocks; based on ovendry weight.

TTF is time-to-failure in minutes and seconds (M:S)

Fail X-sect is the percentage of the finger-joint cross section that failed, based on a visual inspection.

Wood of fail is the percentage of wood failure that occurred in the failure portion of the cross section.

AITC failure type is the mode of failure of the finger joint according to AITC (1992).

Failure zone is the region at which failure was observed in the finger-jointed specimen. Location of the finger joint is equal to 0 in.; values in the negative direction indicate failure in side-A; values in the positive direction indicate failure in side-B. Failure not including the 0-in. location means that failure occurred away from the finger joint.

Notes include comments such as cause of failure; CK is center knot; EK is edge knot; SOG is slope of grain; and GD is grain deviation.

Appendix B—Beam Failure Descriptions

Table B1 lists the details of the individual glulam beam failures. This information includes total time to failure, failure load, an evaluation of whether compression wrinkling in the lumber was observed in the top compression laminations, and a description of the propagation of the failure crack in the beam. Descriptions involving an end joint include the percentage of the end-joint cross section that failed (listed in parentheses), followed by the amount of wood failure in the failure portion of the cross section.

Table B1—Bending test results for the 12 Yellow-Poplar glulam-GFRP beams[a]

Beam	TTF (min)	Failure load (lb)	Compression wrinkling	Beam failure description
1-B	8.51	27,880	Yes, top lam EJ at 13 ft and at midlength, wrinkling in the 2nd lam at midlength	Failed at TL-EJ at 10.2 ft with 20% wood failure: GFRP-wood delaminated completely, GFRP-GFRP bond was intact.
2-B	13.07	28,170	Yes, through top 2 lams at 6.8 ft	Failed at TL-EJ (100%) at 9.7 ft with 40% wood failure: GFRP-wood bond delaminated from 9.7 to 14 ft with 50% wood failure on GFRP surface, GFRP-GFRP bond delaminated from 13 to 16 ft.
3	6.78	18,360	No	Failed in TL-EJ (100%) at 11.2 ft with 10% wood failure and 90% shallow.
4-TB	6.51	23,490	No	Failed in TL-EJ (100%) at 9.8 ft with 20% wood failure: Top GFRP-wood bond delaminated between load points, Bottom GFRP-wood bond delaminated for the whole beam.
5-B	6.11	24,220	Yes, in the top lam 9 to 13 ft	Failed in TL-EJ (100%) with 100% wood failure at 3.2 ft through the 2nd lam in EJ (100%) with 40% wood failure at 5.8 ft: GFRP-wood bond delaminated up to 4 ft from zero end, 4 to 6 ft delamination was observed with 10% wood on GFRP, 6 ft to end intact, GFRP-GFRP bond delaminated from zero to 1 ft, 1 to 10 ft intact, 10 to 15 ft delaminated, 15 to 20 ft intact.
6-B	7.76	28,860	No	Failed in TL-EJ (100%) with 50% good wood failure and 50% shallow failure: GFRP-wood bond is intact between the load points but delaminated from the load points to the supports, GFRP-GFRP bond is intact.
7-TB	8.30	26,510	No	Failed in TL-EJ (85%) with 20% wood failure: Top GFRP did not delaminate, bottom GFRP delaminated for the whole beam with 0% wood failure on the surface.
8-TB	5.76	23,490	No	Failed in TL-EJ (50%) at 8 ft with 40% wood failure: Top GFRP-wood bond delaminated between load points, Bottom GFRP-wood bond completely delaminated.
9-B	6.91	28,620	No	Failed in TL-EJ (100%) at 7 ft with 100% wood failure: GFRP- wood bond delaminated completely with 20% wood on the GFRP surface, GFRP-GFRP bond delaminated between the load points.
10-TB	4.90	23,240	No	Failed in TL-EJ (100%) with 25% good wood failure and 75% shallow failure: Top GFRP-wood bond intact, bottom GFRP-wood bond delaminated for the whole beam.
11-TB	6.71	26,420	No	Failed in TL-EJ (40%) with 40% wood failure: Top GFRP-wood bond intact, Bottom GFRP-wood bond delaminated for the whole beam.
12-TB	6.78	22,510	No	Failed in TL-EJ (100%) with 75% good wood failure and 25% very shallow wood failure: Top GFRP-wood bond intact, Bottom GFRP-wood bond delaminated for the whole beam with 5% to 10% wood on the GFRP surface.

[a]B indicates bottom reinforcement; TB indicates top and bottom reinforcement; TTF is time to failure; TL is tension lamination; EJ is end joint.

Appendix C—Beam Failure Maps

The following figures show the mapped properties of the lumber used to fabricate each glulam beam and a visual description of the failure propagation, which corresponds to the descriptions given in Appendix B. End-joint locations were mapped to the nearest 2 to 3 in., represented by a zig-zagged line. The property listed for each piece of lumber is the MOE measured prior to beam manufacture using a transverse vibration test.

Beam No.1

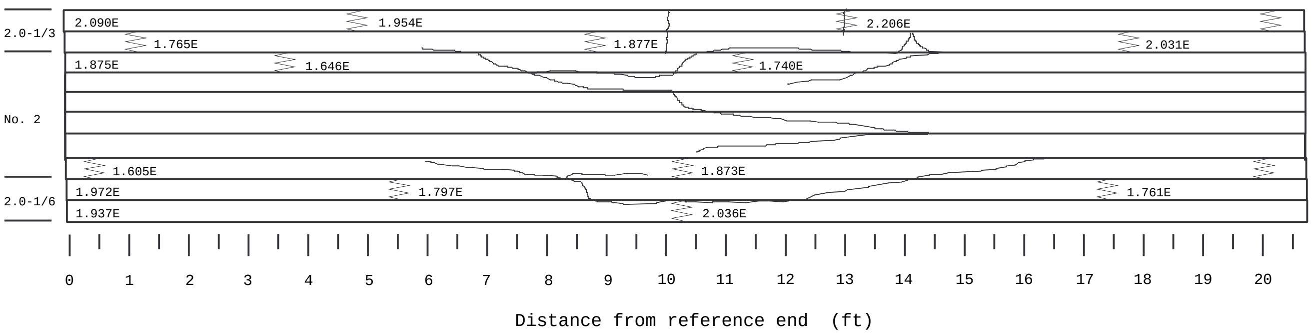

Beam No.2

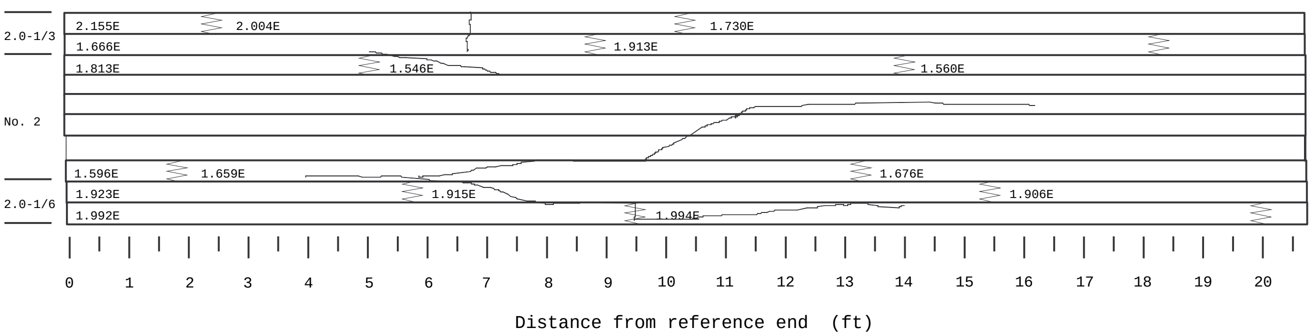

Beam No.3

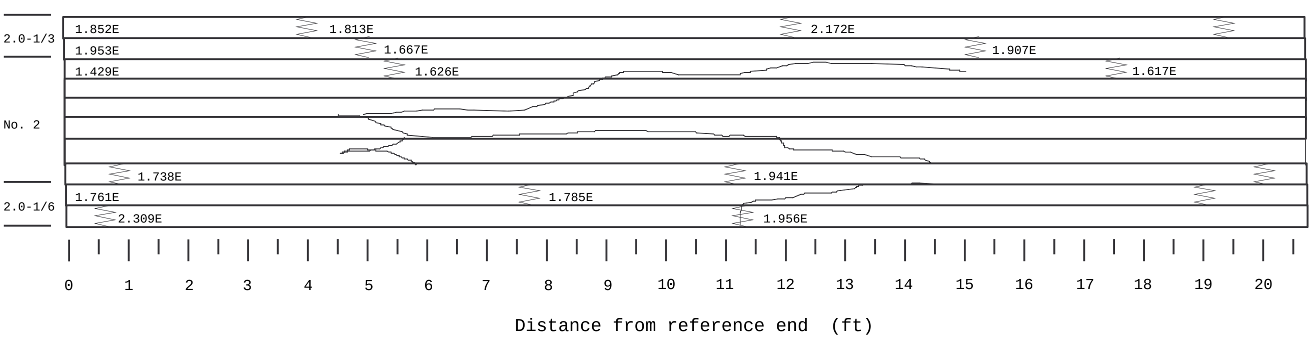

Beam No.4

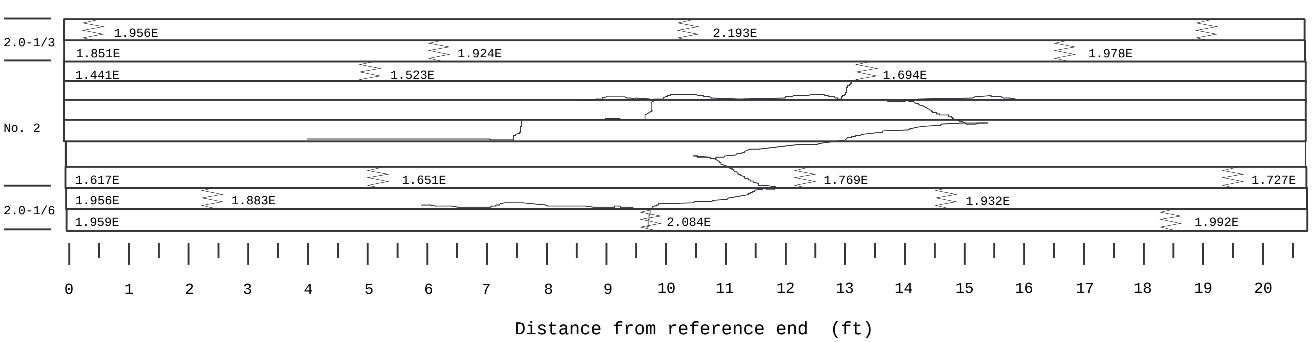

Beam No.5

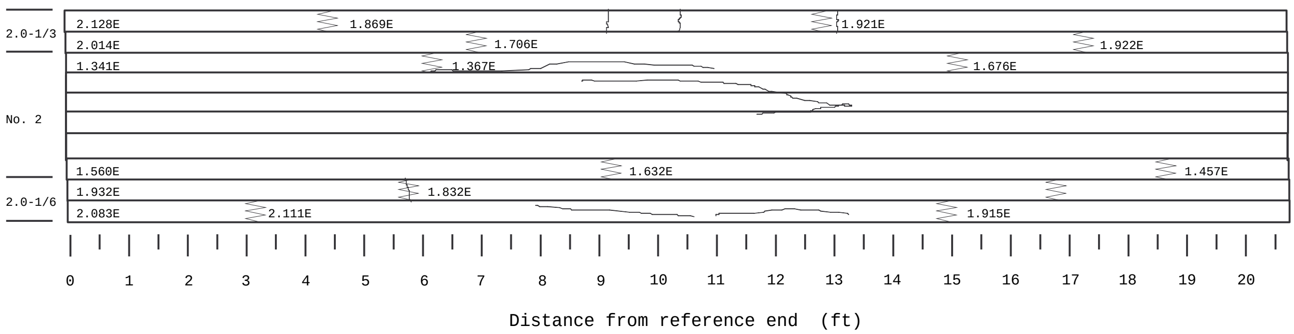

Beam No.6

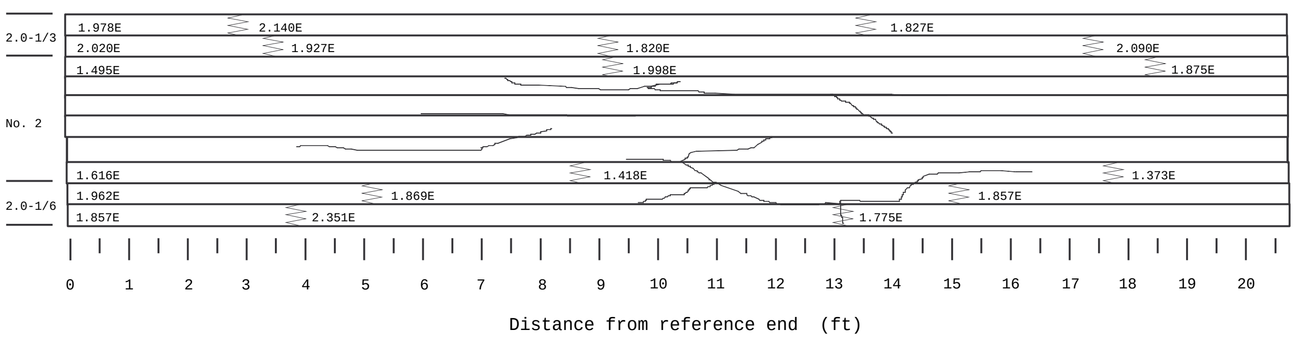

Beam No.7

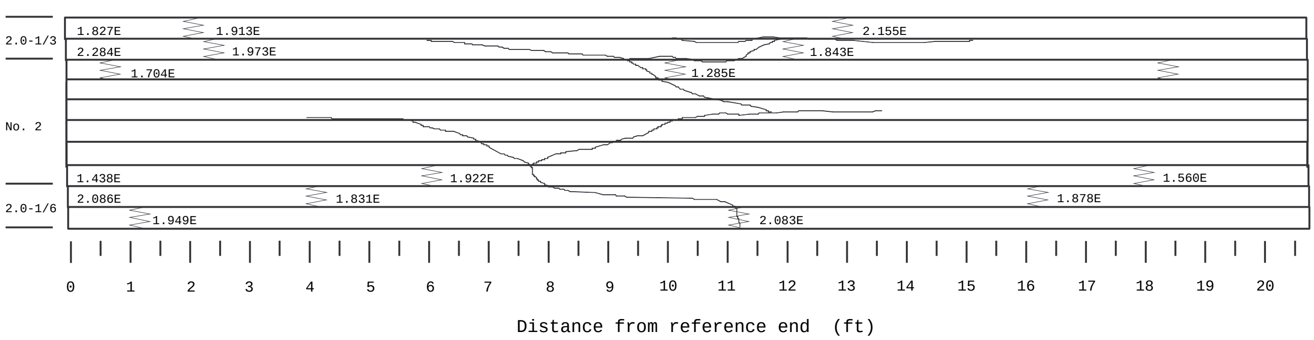

Beam No.8

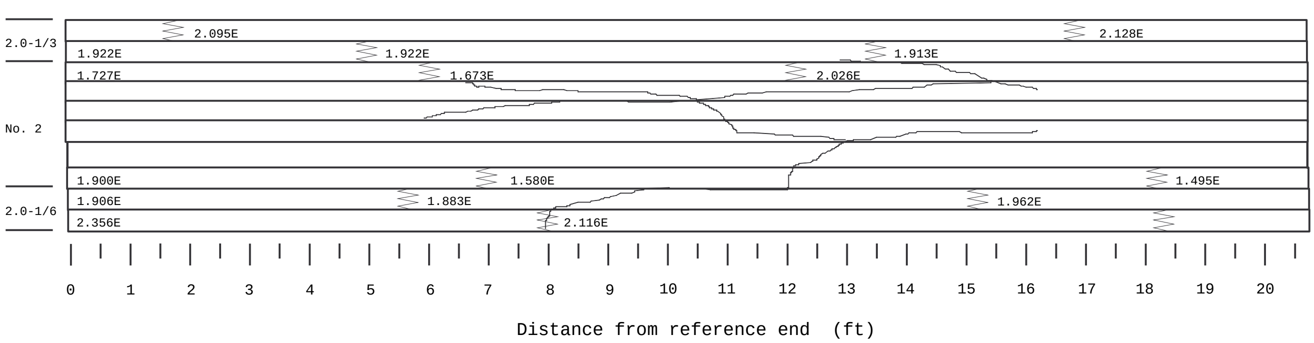

Beam No.9

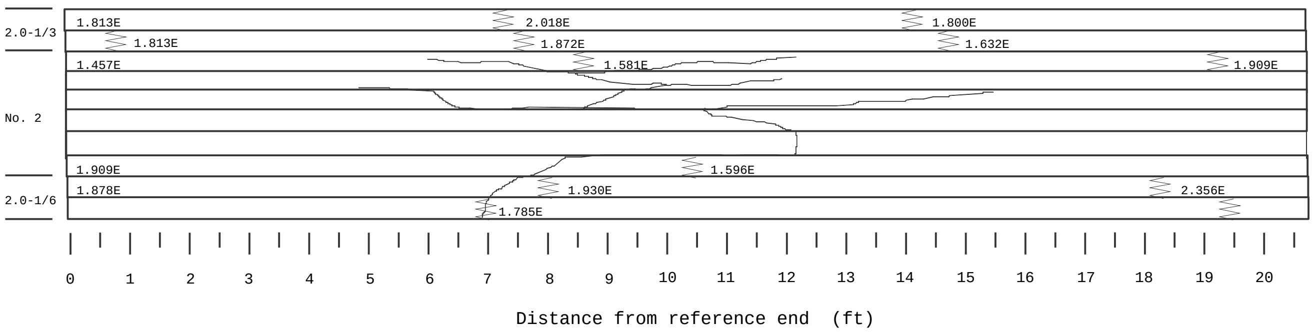

Beam No.10

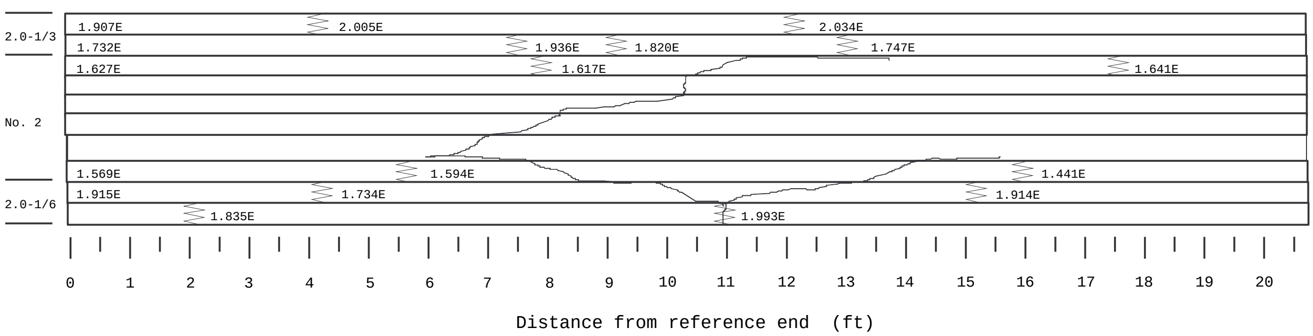

Beam No.11

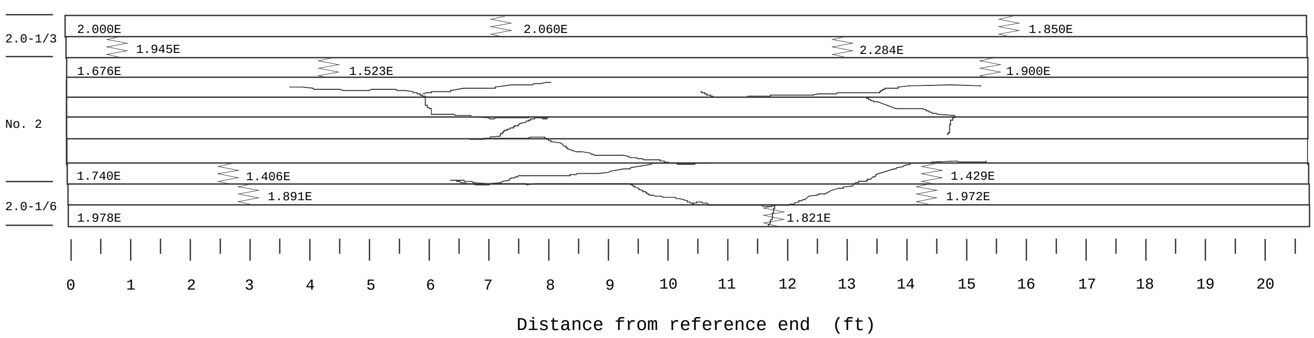

Beam No.12

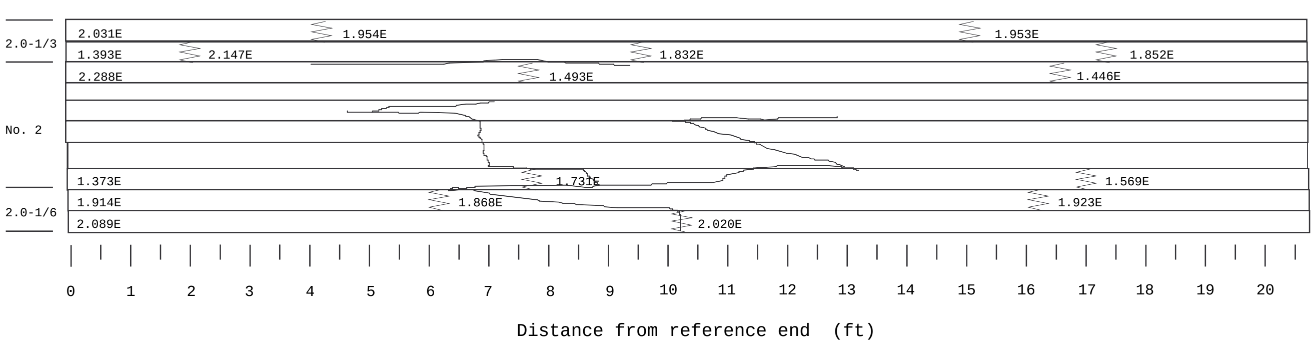

Appendix D—Load–Displacement and Strain–Load

Figures D1 to D24 are paired figures showing results for each glulam beam test. Odd-numbered figures are load–displacement plots, which illustrate the beam deflection at midspan up to failure. Even-numbered figures are strain–load plots at four locations across the beam cross section, taken at the center of the beam length. In these figures, positive-valued strains are tensile, negative-valued strains are compressive. The outermost tensile and compressive strains were measured on the bottom and top of the beam surfaces, respectively. The inner tensile and compressive strains were measured on the side of the beam surface. The exact locations of the strain gages and the calculated slopes of the strain versus load are given in Table 5.

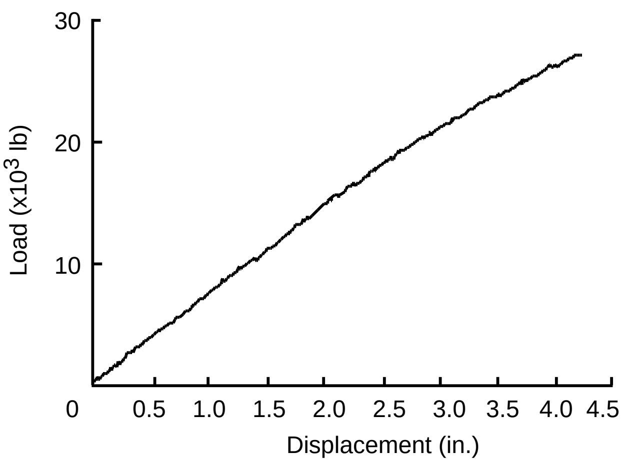

Figure D1—Load–displacement for beam 1.

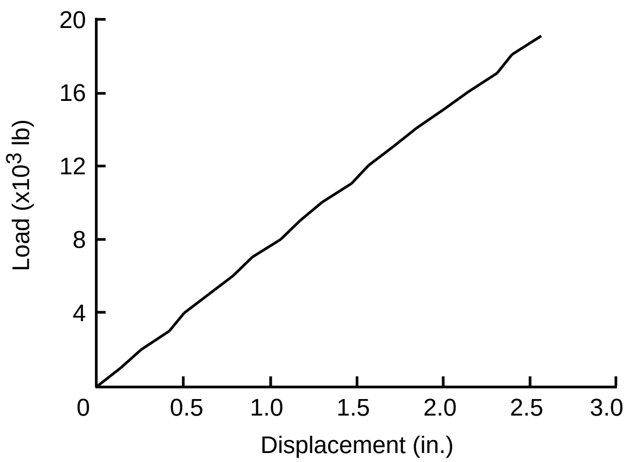

Figure D3—Load–displacement for beam 2.

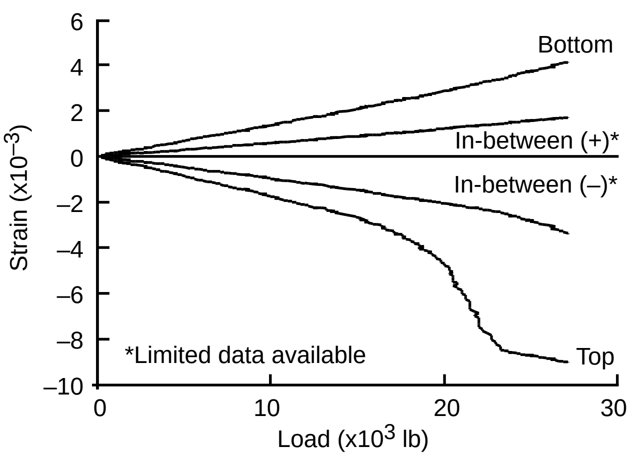

Figure D2—Strain response for beam 1.

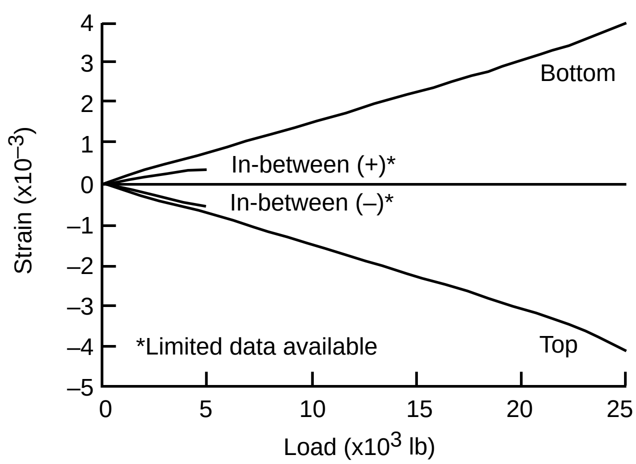

Figure D4—Strain response for beam 2.

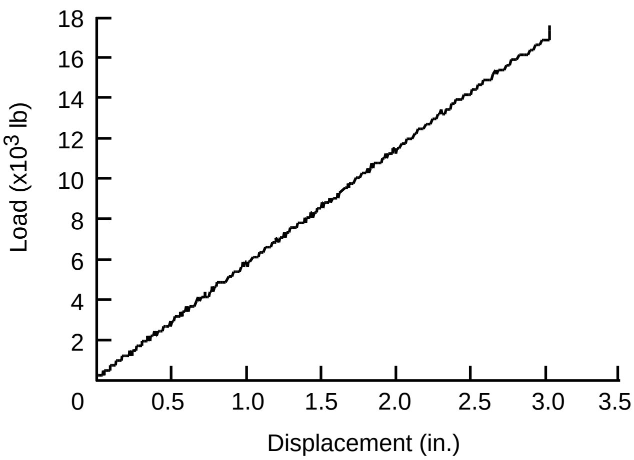

Figure D5—Load–displacement for beam 3.

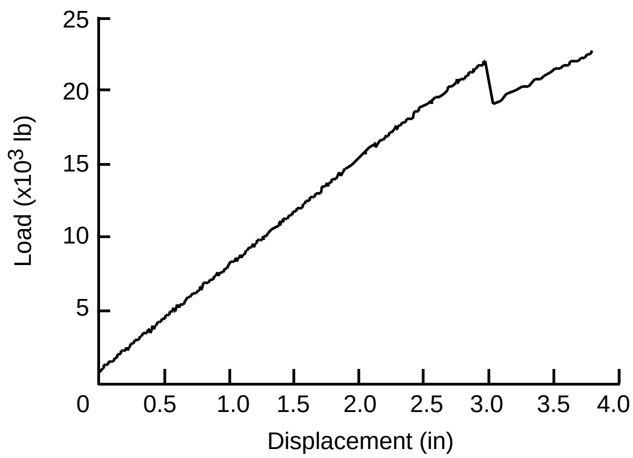

Figure D7—Load–displacement for beam 4.

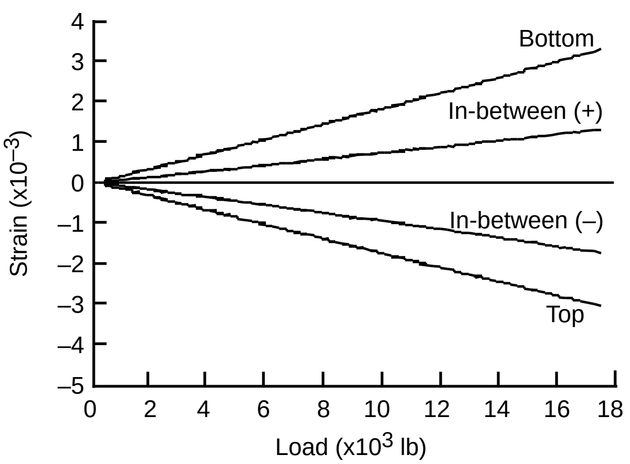

Figure D6—Strain response for beam 3.

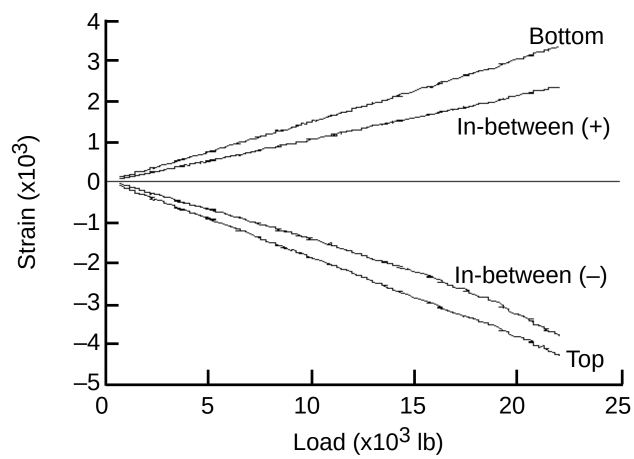

Figure D8—Strain response for beam 4.

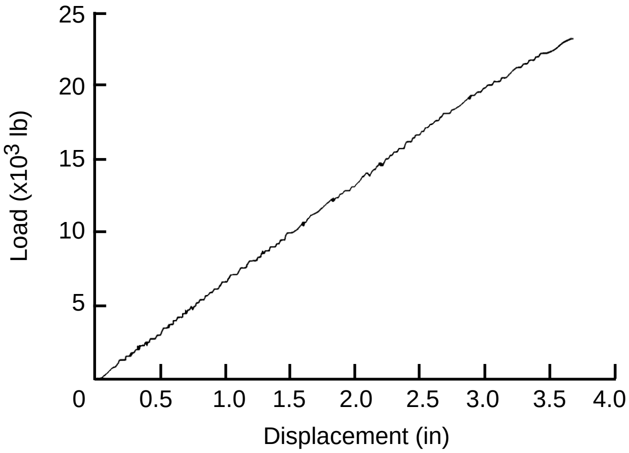

Figure D9—Load–displacement for beam 5.

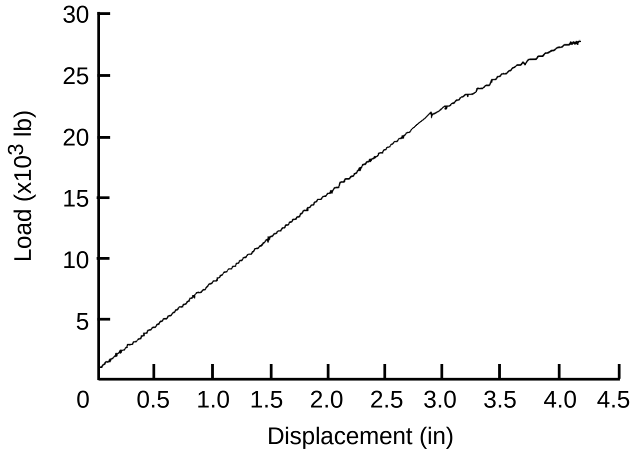

Figure D11—Load–displacement for beam 6.

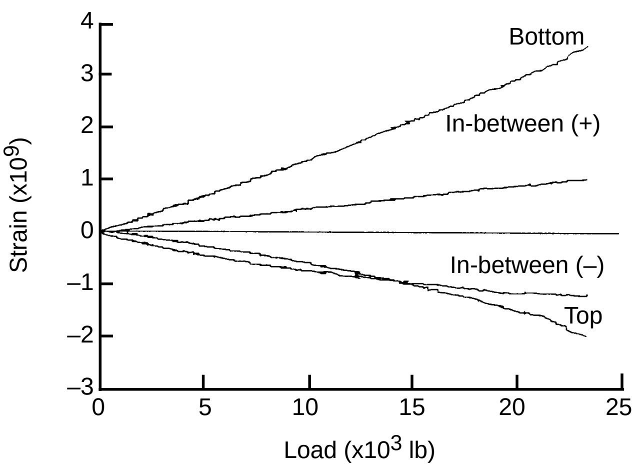

Figure D10—Strain response for beam 5.

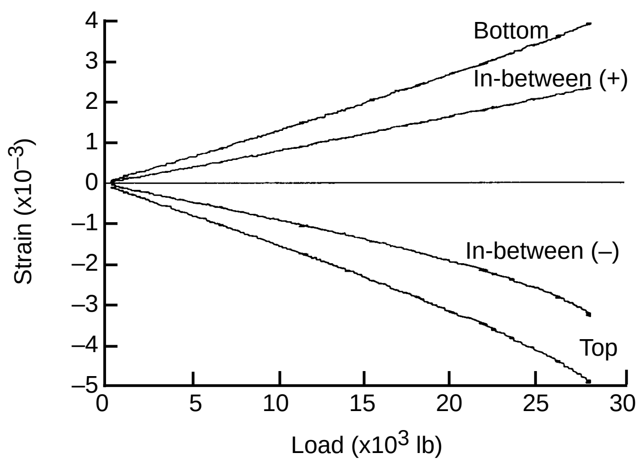

Figure D12—Strain response for beam 6.

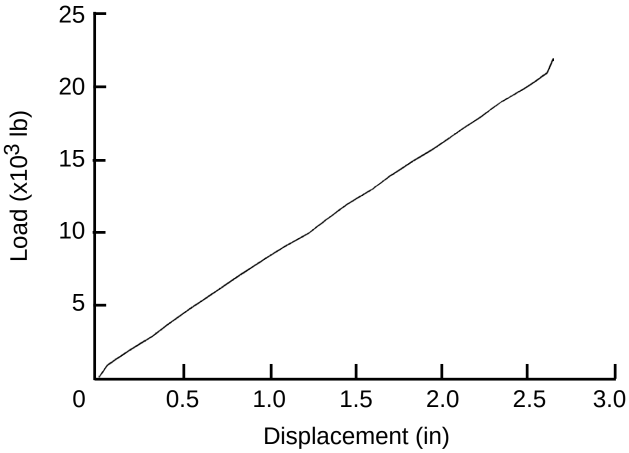

Figure D13— Load–displacement for beam 7.

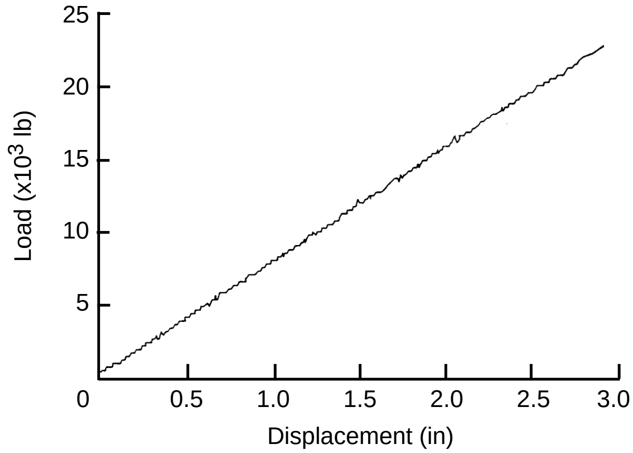

Figure D15— Load–displacement for beam 8.

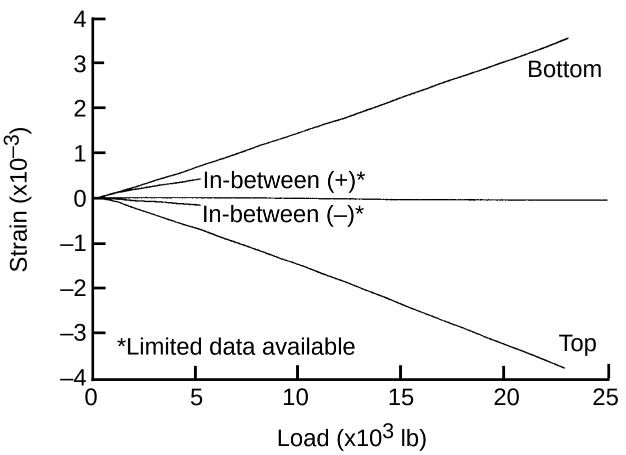

Figure D14—Strain response for beam 7.

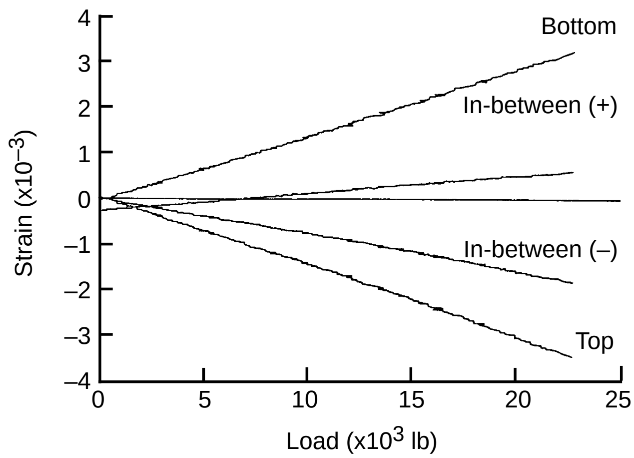

Figure D16—Strain response for beam 8.

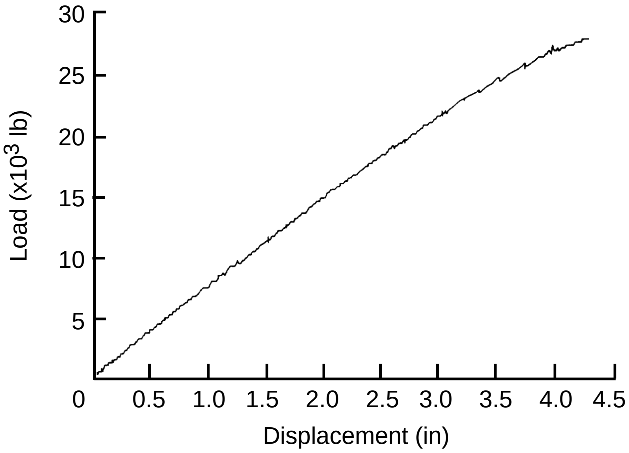

Figure D17— Load–displacement for beam 9.

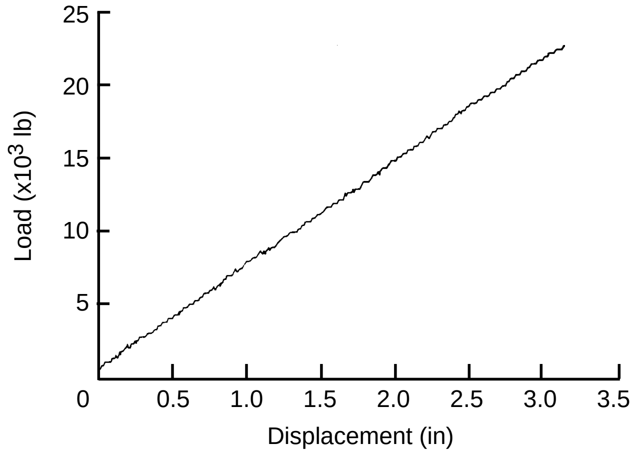

Figure D19—Load–displacement for beam number 10.

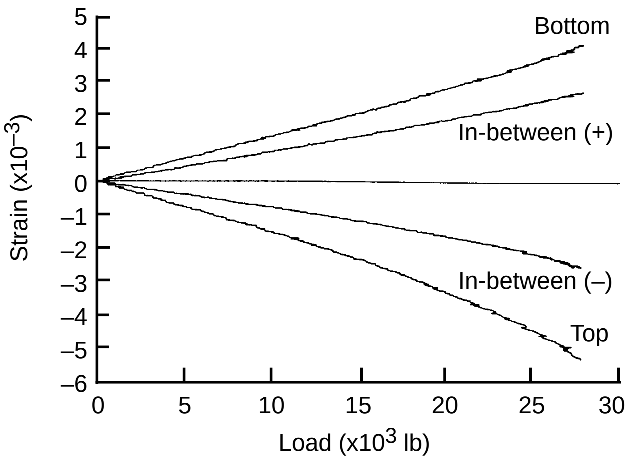

Figure D18—Strain response for beam 9.

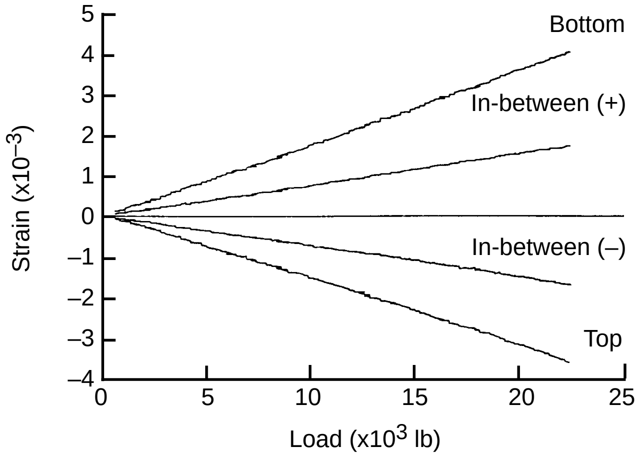

Figure D20—Strain response for beam 10.

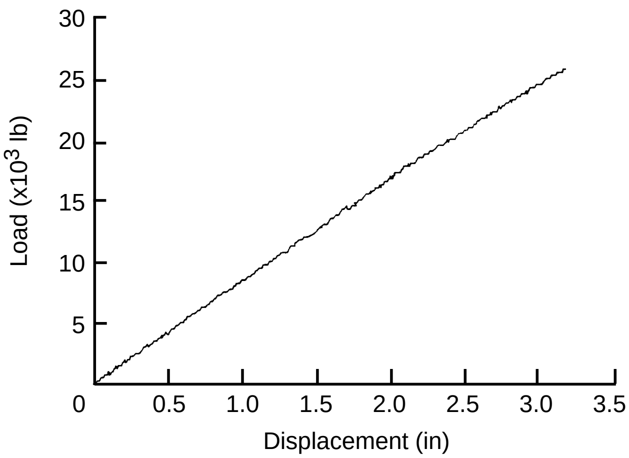

Figure D21—Load–displacement for beam number 11.

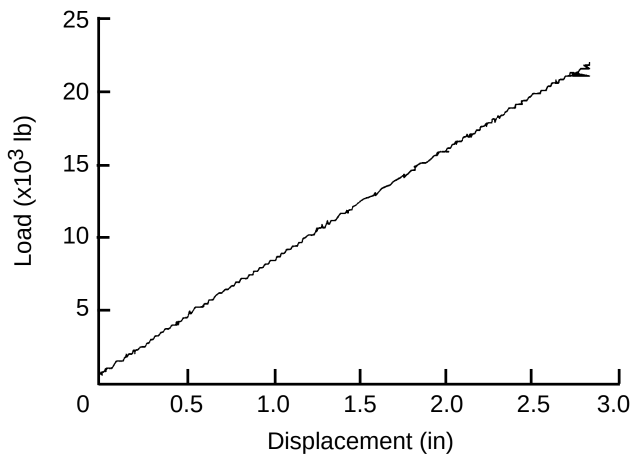

Figure D23—Load–displacement for beam 12.

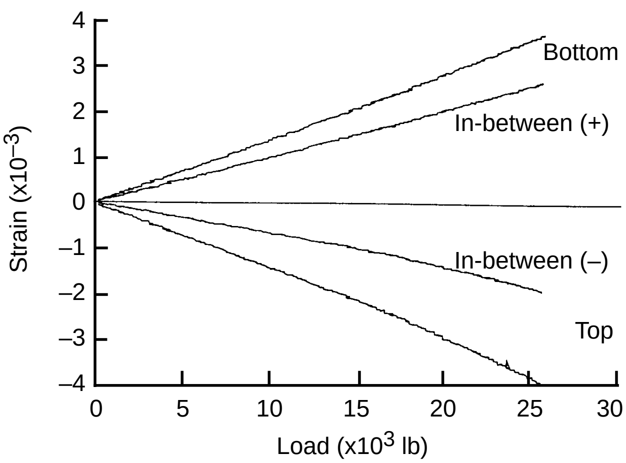

Figure D22—Strain response for beam 11.

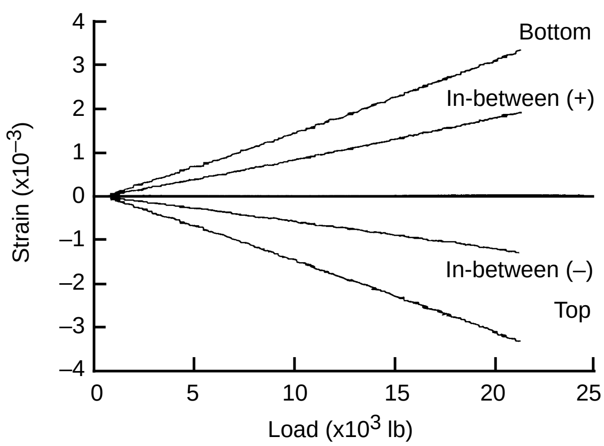

Figure D24—Strain response for beam 12.